Mechanical Properties of Polymers at Ultrasonic Frequencies

BY WARREN. P. MASON AND H. J. McSKIMIN

(Manuscript received October 25, 1951)

Since the mechanical properties of solid polymer materials are largely dependent on the motions that segments of the polymer chains can undergo, to understand these properties one must use measuring techniques which can determine these motions. One of the most promising methods is to measure the reaction of polymer materials to longitudinal and shear waves over a frequency spectrum wide enough to determine the relaxation frequencies due to thermal motions of the principle elements of the chain. The presence of relaxations is indicated by a dispersion in the velocity and attenuation constants of the material, or a dispersion in the characteristic impedance of the material if the attenuation is too high to allow velocity measurements. A number of different types of measuring methods are described in this paper which make possible propagation and impedance measurements not only in solid polymers, but also in liquid polymers and in solutions of polymer molecules in typical solvents.

When these techniques are applied to long chain polymers in dilute solutions, the three relaxations observed correspond to motions occurring in isolated molecules since as the dilution increases, the molecules seldom touch. The lowest relaxation corresponds to a configurational relaxation of the molecule as a whole, the highest relaxation corresponds to the twisting of the shortest segment—containing about 40 repeating units—while the intermediate relaxation corresponds to a transient entanglement of chain segments. All three types of relaxations are present in pure polymer liquids but are spread out over a frequency range due to the perturbing effect of near neighbors of adjacent chains. The high frequency shortest chain relaxation can be traced in solid polymers of the linear chain type such as polyethylene and nylon and produces rubber-like response to mechanical shocks of very short duration.

I. INTRODUCTION

The mechanical properties of solid polymer materials are largely determined by what motions, parts or segments of the polymer chains can undergo. Toughness, mechanical impact strength and ultimate elongation depend on the facility with which the polymer molecule can be displaced.

If only a small motion of the polymer chain can occur within the time of the measurement, the material has high elastic stiffness coefficients and acts similar to a rigid solid. On the other hand, if significant segments of the polymer chain can move at the frequency of measurement, the elastic stiffness is much lower and rubber-like behavior results. An intermediate case, which occurs when the significant motion of the polymer molecule is near the relaxation time at the frequency of measurement, is that of a damping material such as butyl rubber. Even "long time" qualities of plastics such as creep, stress relaxation and recovery depend on the integrated displacements of rapidly oscillating segments of the chain.

One of the most promising methods for investigating these motions is to determine the reaction of mechanical waves on the polymer materials over a wide spectrum of wavelengths, eventually going to frequencies comparable with those of thermal vibrations of significant groups or segments in the macromolecules.

If one wishes to understand the origins of these motions it is necessary to measure the molecules in the form of liquids or solutions since then the segments of the molecule are less restrained by their neighbors and can perform all the possible vibrations. Polymer liquids are also interesting in themselves as sources of damping material. To apply these results to rubbers and solid materials, one then has to measure the modifications of the polymer chain motion caused by the close approach of near neighbors, by measuring the mechanical properties of these materials.

By using different types of techniques, these processes can be applied to molecules in solution, to liquid polymers and to solid polymers. The principal types of methods used for liquids are the torsional crystal, the torsional wave propagation system and the shear wave reflectance method, all of which are described in Section II. For solids an optical method and an ultrasonic method are described in Section V. All of these methods involve displacements of 10^{-6} cm or less so that non-linear effects are negligible.

All of these methods depend on setting up shear or longitudinal waves in the medium and observing either the velocity and attenuation of the wave, or the reaction of the medium back on the properties of the transducer. If the attenuation of a wave in the medium under consideration is low enough to permit the wave parameters, i.e., the velocity and attenuation per wavelength to be determined, the relaxation of some significant part of the polymer molecule is determined by the dispersion of the wave properties which occur, as shown by Fig. 1A, in the form of an increase in velocity and a maximum in the attenuation per

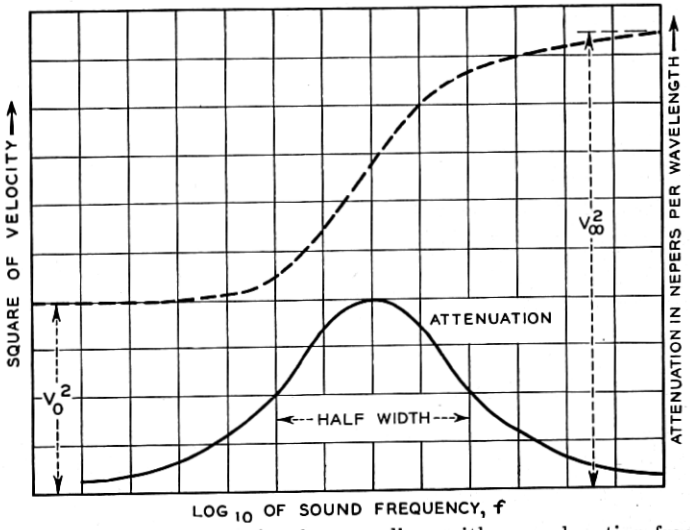

Fig. 1A—Velocity and attenuation for a medium with one relaxation frequency.

wavelength curve. If the variation in this relaxation mechanism is studied as a function of temperature and chain length, the type of segment may be determined. If, however, the attenuation of the medium is so high that its wave properties cannot be determined, some information can still be obtained by determining the loading, or mechanical impedance, that such a wave exerts on the driving crystal or transducer. If all the relaxations occur in the stress-strain relation, it can be shown that there is a reciprocal relation between the propagation constant $\Gamma = A + jB$, and the characteristic impedance per square centimeter Z_0 given by the equation

$$Z_0\Gamma = (R + jX)(A + jB) = j\omega\rho \tag{1}$$

where A is the attenuation and B the phase shift per centimeter, R the mechanical resistance and X the mechanical reactance per square centimeter, ω is 2π times the frequency and ρ the density of the medium. A typical two relaxation mechanism[1] is shown by the curves of Fig. 1B. By assuming values for the stiffness and dissipation factors and fitting a theoretical curve to the measured values, the relaxation frequency or frequencies can be determined.

[1] All the relaxation mechanisms discussed in this paper are represented in terms of equivalent parallel electric circuits in which the resistance terms represent viscosities and the inverse of capacities represent shear elastic stiffnesses. In mechanical terms these correspond to a series of Maxwell models as discussed in a paper by Baker and Heiss to be published in the next issue.

The most information about the motions of isolated polymer chains can be obtained by investigating the properties of polymer solutions. This follows from the fact that in pure polymer liquids, and in solids, the mechanical properties are mainly determined by interactions between chains on account of the close packing of the chains. If, however, one dissolves the polymer molecules in a solvent, the inter-chain and intra-chain reactions can be separated as the dilution increases. When the polymer is in the order of one percent of the solvent, the chains on the average touch very seldom and the mechanical properties of the solution are determined by the properties of single molecules. As discussed in Section III, three types of chain segment motion have been isolated, (1) a configurational relaxation of the chain as a whole, (2) a position change of the shortest segment and (3) twisting of the shortest chain segment. Above the frequency of relaxation of this chain segment the joints of the polymer molecule become frozen and the chain becomes very stiff. These shortest chain relaxations occur also in pure polymer liquids, in rubbers and in non rigid solids with linear chain segments such as polyethylene. In pure liquids a lower frequency quasi-

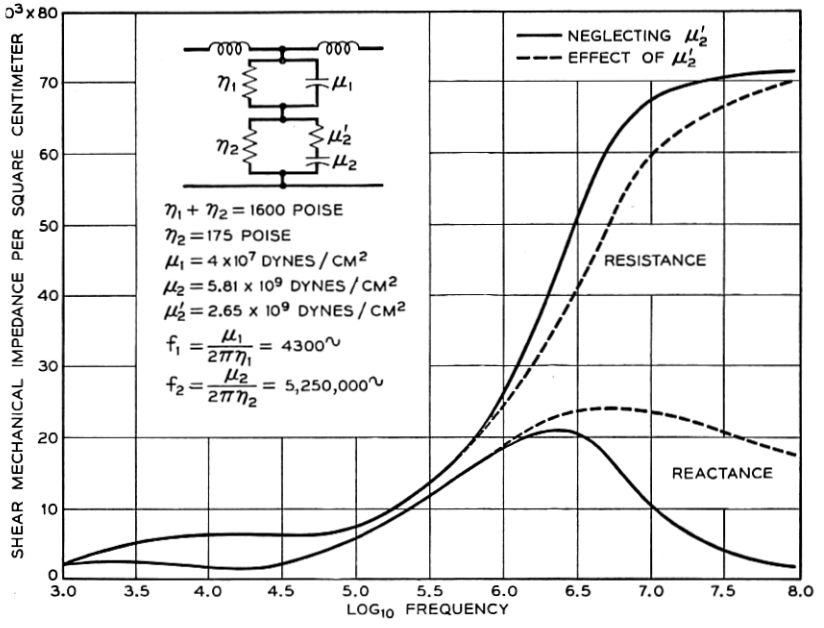

Fig. 1B—Mechanical impedance loading for a medium with two relaxation frequencies.

configurational relaxation also occurs for chain lengths greater than 60 elements but for chain lengths less than 40 elements this type of relaxation disappears. From the difference between the high frequency shear elasticities measured for polyethylene and nylon 6-6 and those measured for static pulls, it appears that there may be lower frequency relaxations in these materials as well.

II. METHODS OF MEASUREMENT FOR SOLUTIONS AND PURE POLYMER LIQUIDS

To measure the mechanical properties of such dilute solutions, shear waves have been used since for longitudinal waves the added stiffness caused by the dissolved polymers is very small compared to the stiffness of the solvent alone. The velocity and attenuation of a longitudinal wave are given by the equations

$$v = \sqrt{\frac{\lambda + 2\mu}{\rho}}; \qquad A = \frac{2\pi^2 f^2}{\rho v^3}[\chi + 2\eta] \tag{2}$$

where λ and μ are the Lamé elastic constants, f the frequency, ρ the density, v the sound velocity, χ the compressional viscosity and η the shear viscosity. Since for a one percent solution of polyisobutylene in cyclohexane the shear elasticity does not exceed 90,000 dynes/cm^2, whereas the value of λ is in the order of 2×10^{10} dynes/cm^2, it is obvious that the longitudinal velocity would have to be measured to an accuracy of 1 part in 100,000 before the presence of polymer molecules could be ascertained. Attenuation measurements give some information on the added viscosity due to the chain molecules but since longitudinal attenuations are not easily measured below 1 megacycle, the most interesting frequency range is missed.

A pure shear wave in a viscous liquid is propagated according to the equation[2]

$$v = v_0 e^{-\sqrt{\frac{\pi f \rho}{\eta}}(1+j)z} \tag{3}$$

where v is the transverse particle velocity, ρ the density, f the frequency, η the shear viscosity, $j = \sqrt{-1}$ and z the distance. For typical solvents, the attenuation is so high that wave motion cannot be measured. However the viscous wave produces an impedance loading on a crystal generating such a wave which can be measured by the change in the resonant frequency and the change in the resistance at resonance. The mechanical impedance per square centimeter caused by such a viscous

wave is equal to[2]

$$Z_0 = \sqrt{\pi f \eta \rho}\,(1 + j) = R_M + jX_M \tag{4}$$

This causes a change in resistance, and a change in frequency in a crystal generating a shear wave in the liquid equal to

$$\Delta R_E = K_1 R_M; \qquad \Delta f = -K_2 X_M \tag{5}$$

where K_1 and K_2 are constants of the crystal which can be obtained approximately from the dimensions and piezoelectric constants of the crystal but which are more accurately obtained by calibration in known liquids. The constants K_1 and K_2 vary slightly with temperature and should be calibrated over a temperature range.

The first instrument to use a vibrational method for measuring viscosity was the vibrating wire method of Phillipoff.[3] In this method a wire was vibrated in a liquid and the damping rate was used as a measure of the viscosity. Another method also applicable in the low frequency range is the transducer method of Ferry.[4] In this method wires are vibrated by electromagnetic transducers and the resistance and reactance drag on the wires are measured by the change in the electrical resistance and reactance of the transducer. From the constants of the transducer, the equivalent viscosity and stiffness of the liquid can be measured.

In the medium frequency range a torsional crystal[5] method was devised by one of the writers which has been applied in the frequency range from 10 to 150 kc. The torsional crystal is shown by Fig. 2. For these types of measurements the crystal usually is made of quartz with four electrodes of gold evaporated on the surface. Four wires are soldered on the surface and serve as supports as well as electrodes. The motion is all tangential to the surface and tests at Bell Laboratories and at the Franklin Institute,[6] where a precision study of the torsional crystal has been made, have shown no observable longitudinal waves from the crystal surface. The process of measurement consists in measuring the

[2] W. P. Mason, *Piezoelectric Crystals and Their Application to Ultrasonics*, D. Van Nostrand, 1950, p. 340.

[3] W. Phillipoff, *Physik. Zeits*, **35**, 1934, pp. 884–900.

[4] T. L. Smith, J. D. Ferry and F. W. Schemp, "Measurement of the Mechanical Properties of Polymer Solutions by Electromagnetic Transducers," J. App. Phys., **20**, No. 2, Feb. 1949, pp. 144–153.

[5] W. P. Mason, "Measurement of the Viscosity and Shear Elasticity of Liquids by Means of a Torsionally Vibrating Crystal," A.S.M.E., **69**, May 1947, pp. 359–367.

[6] P. E. Rouse, Jr., E. D. Bailey, and J. A. Minkin, "Factors Affecting the Precision of Viscosity Measurements with the Torsional Crystal," Laboratories of the Franklin Inst., Report 2048, presented to Am. Petroleum Inst., May 4, 1950.

resonant frequency and resonant resistance of the crystal in a vacuum, then introducing the solution to be measured, the change in the resonant resistance ΔR_E and the change in resonant frequency Δf are determined by an electrical bridge. Several short cuts are possible if the mechanical impedance is not too high. By measuring the capacity at a frequency considerably higher than the crystal frequency, the resistance at resonance and Δf can be obtained by changing the frequency and resistance until a balance is obtained leaving the capacity unchanged. This method has been used to measure viscosity, and a recent precision study at the Franklin Institute[6] has shown that it agrees with other methods to an accuracy of well under a per cent.

The torsional quartz crystal has been successfully used to measure liquids having a viscosity up to 10 poise, but above this viscosity the electrical resistance gets so high that it is hard to measure it since it is shunted by the much smaller reactance of the static capacitance of the crystal. A crystal of higher electromechanical coupling such as am-

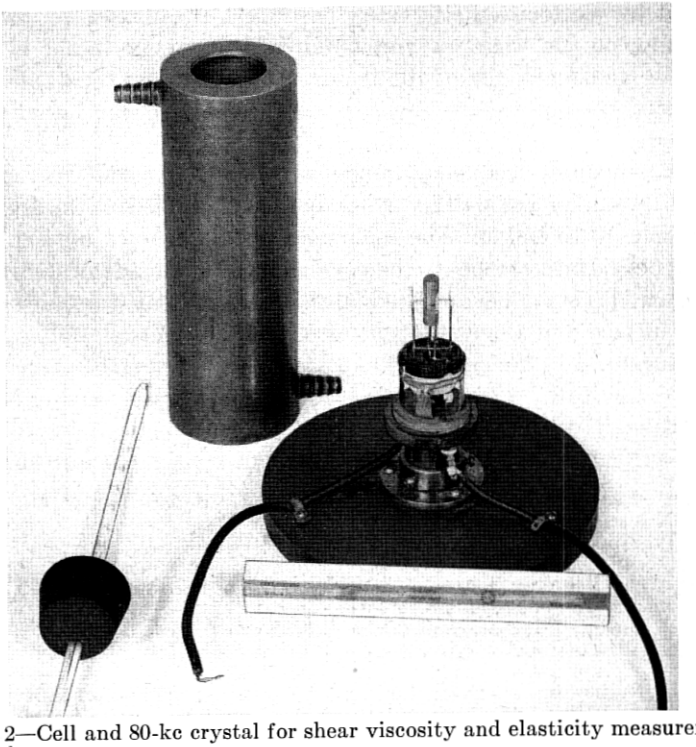

Fig. 2—Cell and 80-kc crystal for shear viscosity and elasticity measurements of liquids.

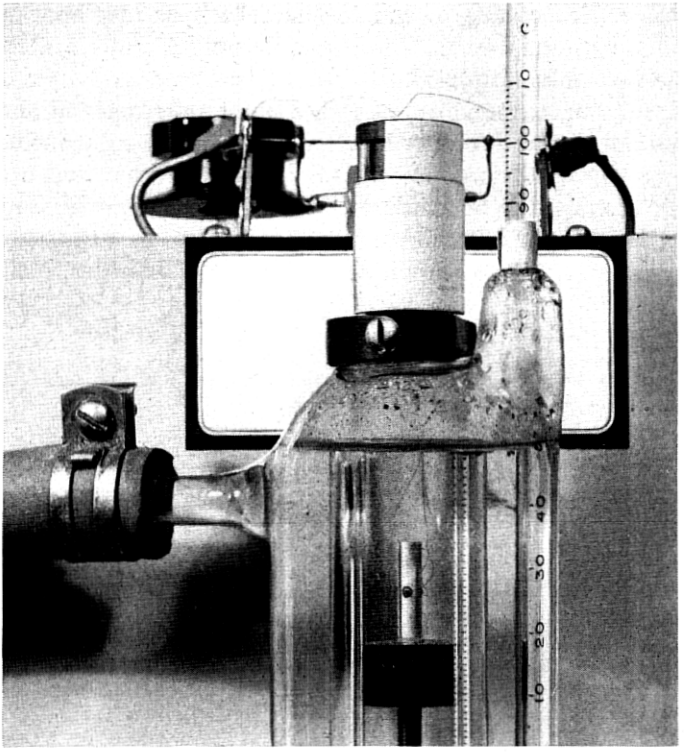

Fig. 3—Photograph of torsional crystal and rod.

monium dihydrogen phosphate (ADP) will cause the electrical resistance component to be smaller in comparison to the reactance of the static capacitance and hence can be used to measure higher viscosities. However, since wires cannot be soldered to the surface but must be glued, the crystal is much more fragile than quartz and its use has been abandoned in favor of another method which makes use of the phase and attenuation change in a torsional wave in a rod caused by the surrounding liquid whose properties are to be measured.

This method, devised by one of the writers,[7] consists in sending a short train of torsional waves, periodically repeated, down a glass or metal rod. As shown by Fig. 3, the torsional wave is generated by a torsional quartz crystal soldered or glued to the end of the rod. These waves travel to the free end of the rod and are reflected back to the crystal where they are detected, amplified, and displayed on a cathode ray

[7] This method is described by H. J. McSkimin, in a paper before the Acoustical Soc. of Am. in October, 1951.

oscilloscope. Echoes due to end to end reflections also appear, being attenuated by normal acoustic losses until they are undetectable by the time the next pulse is applied.

With only air surrounding the rod, a phase reference and amplitude reference are obtained for the first received wave (or subsequent echoes if greater sensitivity is desired). The rod is then immersed a definite length in the liquid to be measured, as shown in Fig. 4, with a resulting phase retardation and amplitude reduction. These are measured by employing the experimental circuit shown by Fig. 5. In order to allow the

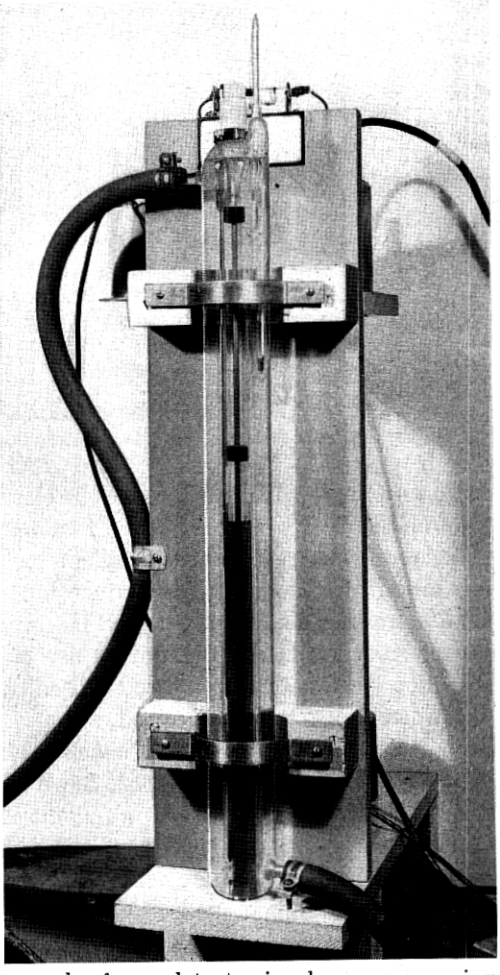

Fig. 4—Photograph of complete torsional wave measuring equipment.

use of one crystal for both receiving and transmitting, the crystal is put in the bridge circuit of Fig. 5 where a resistance and capacity are used to balance out the transmitted pulse so that it will not overload the amplifier. The relatively weak voltages generated by the incoming acoustic waves pass through directly. The gate circuit provides pulses of radio frequency voltage at repetition rates in the range of 20 to 100 per second with a synchronizing voltage supplied to the oscilloscope for the horizontal sweep. The frequency range of the device is from 20 to 200 kc. Both glass and nickel-iron rods were used, the latter having a very low frequency-temperature coefficient. With a 100-kc quartz

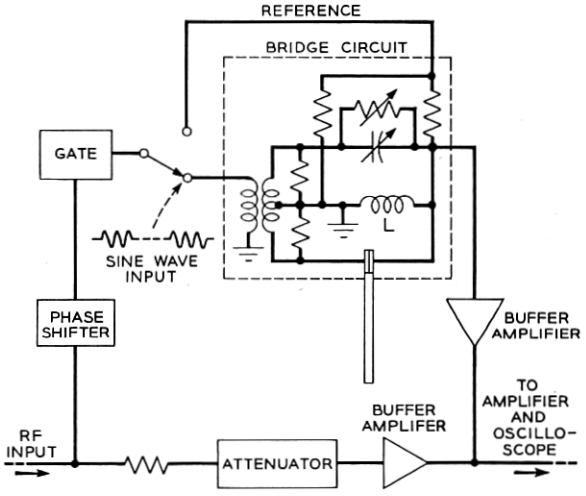

Fig. 5—Experimental pulsing circuit for measuring torsional impedance of liquids.

torsional crystal, a rod length of 21 inches and diameter of 0.2 inch were used. The entire crystal-rod assembly is placed inside a glass temperature control unit, as shown by Fig. 4, through which water can be circulated to provide temperatures in the range 0°C to 80°C. The test liquid is placed either directly into the inner bore of this water jacket, or in another tube which can be inserted from the bottom to surround the rod up to a fixed mark.

In use, both phase and attenuator settings were adjusted to balance the first received pulse against the continuous wave component passing through the attenuator. Cancellation for the duration of the pulse was visually indicated on the oscilloscope. A plot of balance phase and level is made as a function of the temperature. When the liquid is introduced an attenuation change $\overline{\Delta A}$ and a phase change $\overline{\Delta B}$ are required to

re-balance the circuit. These are measured by the amount of attenuation in nepers (1 neper = 8.68 db) and the number of radians phase shift required to re-establish a balance. An alternate method of measuring phase shift is to measure the change in frequency required to re-establish balance. If this method is used the phase shift change of the overall circuit with frequency has to be calibrated for the uncovered rod by

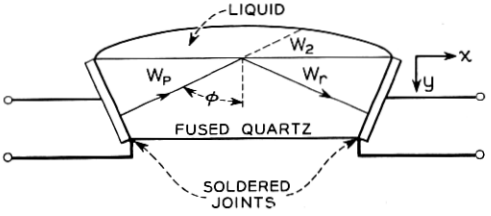

Fig. 6—High frequency shear reflection method for measuring shear impedances of liquids.

noting the frequencies for which 360° phase shifts (as measured by balance) occur in the circuit.

It is shown in the appendix that the torsional impedance of the liquid per square centimeter is given by

$$Z = \left(\frac{\rho v_0}{4}\right)\frac{a}{\ell}\left[\overline{\Delta A} + j\overline{\Delta B}\right] \tag{6}$$

where ρ is the density, and v_0 the sound velocity in the rod, a is the radius and ℓ the covered length of the rod and $\overline{\Delta A}$ and $\overline{\Delta B}$ are respectively the change in attenuation in nepers and the change in phase shift in radians to re-establish balance. If a very viscous liquid is used it may be necessary to correct for the fact that the torsional impedance may differ from the plane wave impedance as discussed in the appendix.

This device can measure liquids having dynamic viscosities from 10 poise to 1,000 poise with an accuracy of the order of 10 per cent. The frequency range covered may be from 20 to 200 kc depending on the size of the crystal used to drive the rod. Hence it supplements the torsional crystal method for very viscous liquids.

At frequencies above 500 kc, the torsional crystal becomes too small to be used practically and recourse is had to a high frequency pulsing method.[8] As shown by Fig. 6, shear waves are set up in a fused quartz

[8] W. P. Mason, W. O. Baker, H. J. McSkimin and J. H. Heiss, "Measurements of the Shear Elasticity and Viscosity of Liquids by Means of Ultrasonic Shear Waves," Phys. Rev., **75**, No. 6, March 15, 1949, pp. 936–946. See also H. T. O'Neil, "Refraction and Reflection of Plane Shear Waves in Viscoelastic Media," Phys. Rev., **75**, No. 6, March 15, 1949, pp. 928–936.

rod by means of a Y-cut or AT cut crystals soldered to a silver paste layer baked on the fused quartz surface. The particle motion of the shear wave is parallel to the large reflecting surface and hence only shear waves are reflected from this surface. These impinge on a second shear crystal which is connected to an amplifier and oscillograph. Since the attenuation in fused quartz is so low, a long series of reflected pulses appear on the oscillograph. When a liquid, whose shear properties are to be measured, is placed on the fused quartz surface, this causes a change in the amplitude and phase of the reflected wave. By using the balance method shown by Fig. 7, in which two identical fused quartz rods are used, one of which has a liquid layer and the other does not, and by using a phase shifting network and an attenuator to balance out

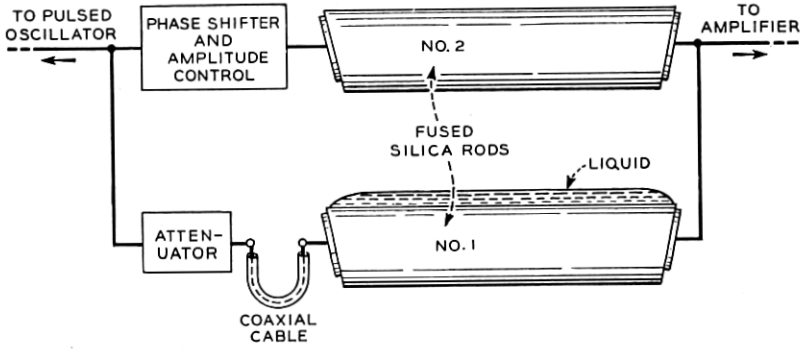

Fig. 7—Method for obtaining resistance and reactance terms for high frequency shear reflection method.

pulses, the shear impedance of the liquid can be determined. If R is the loss per reflection expressed as a current ratio, θ the change in phase angle required to rebalance the circuit and φ the angle between the wave normal and the reflecting surface, it can be shown[8] that the shear impedance of the liquid is

$$Z_M = R_M + jX_M = Z_q \cos \varphi \left[\frac{1 - R^2 + 2jR \sin \theta}{1 + R^2 + 2R \cos \theta}\right] \tag{7}$$

where Z_q is the impedance ρv for shear waves in the quartz. This is equal to

$$Z_q = 2.20 \times 3.76 \times 10^5 = 8.27 \times 10^5 \text{ mechanical ohms}$$

Since this impedance is much larger than that of the liquids that are to be measured, the sensitivity is increased by making φ large. In practice φ was taken as 80°. This method is applicable from 3 mc up to 100 mc

and complements the other methods. Fig. 8 shows a photograph of the equipment.

III. MEASUREMENTS OF POLYMERS IN SOLUTION

When such methods are applied to a polymer solution, it is found that the resistance and reactance components are no longer equal but the resistance is invariably larger than the reactance. This indicates the presence of a shear elasticity in the solution. If the molecules have a single relaxation frequency, it has been found that the shear properties of the liquid can be represented by a stress-strain equation of the type

$$T = \eta_A \frac{\partial S}{\partial t} + \frac{1}{\dfrac{1}{\eta_B \dfrac{\partial S}{\partial t}} + \dfrac{1}{\mu_B S}} \tag{8}$$

where T is the shearing stress, S the shearing strain, η_A the solvent viscosity, η_B a molecular viscosity of some particular motion of the chain which disappears when the reactance of the chain stiffness μ_B of this motion is low enough so that the motion can follow the applied shearing stress at the frequency of the measurement. When this type of mechanism is present in the liquid, it has been shown[9] that the impedance the liquid presents to the crystals is

$$Z_0 = R_M + jX_M = \frac{\rho\mu_B\eta_B^2 + j\left[\omega\rho\eta_A\eta_B^2 + \dfrac{\rho\mu_B^2}{\omega}(\eta_A + \eta_B)\right]}{\eta_B^2 + \mu_B^2/\omega} \tag{9}$$

Fig. 9 shows a plot of the resistance and reactance components of an assumed solution having a single relaxation frequency, and a viscosity 30 times the solvent viscosity. At very low frequencies, the resistance and reactance follow that of a solution, but for frequencies comparable with the relaxation frequency, the resistance becomes larger than the reactance while for very high frequencies the two come together on a line determined by the solvent viscosity. If there is more than one relaxation frequency, the resistance and reactance may coalesce for several intermediate stages. A continuous distribution would give a definite relation between the frequency dependence of resistance and reactance.

The torsional crystal and the shear wave reflection method have been applied to long chains of polyisobutylene dissolved in various sol-

[9] W. P. Mason, *Piezoelectric Crystals and Their Application to Ultrasonics*, D. van Nostrand, 1950, p. 353.

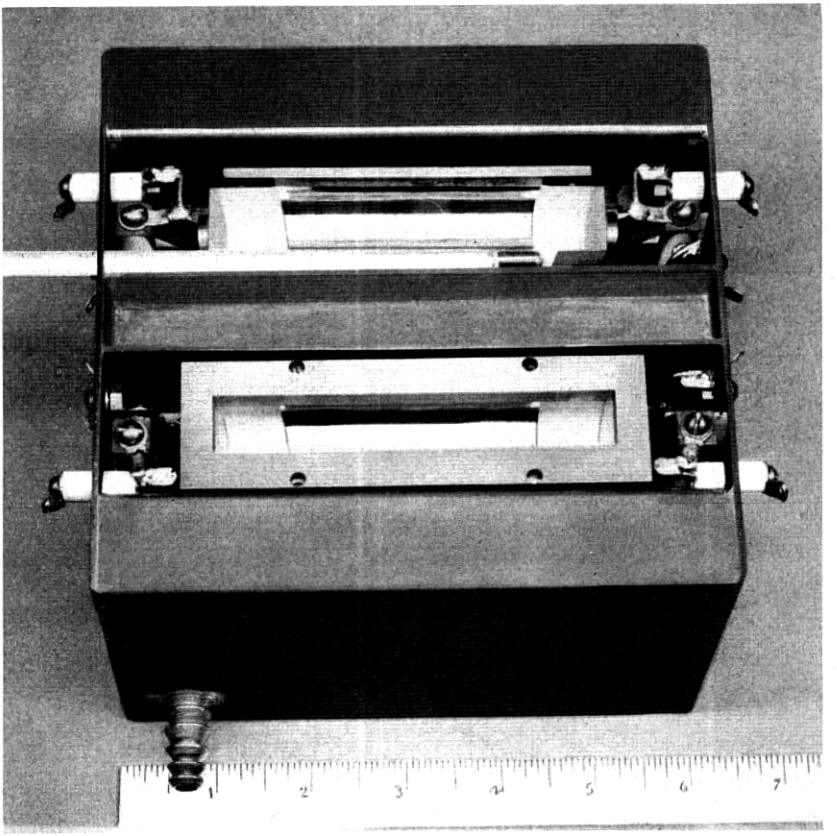

Fig. 8—Dual reflecting block assembly for measuring high frequency shear impedances of liquids.

vents with concentrations ranging from zero per cent to 10 per cent. Polyisobutylene is a polymer molecule having the chemical formula

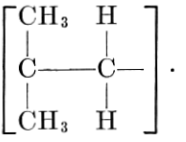

Non-planar zigzag segments can be expected in the liquid state. Fig. 10 shows measured curves for 20 kc of the resistance and reactance for solutions of viscosity average molecular weight of 3,930,000 in cyclohexane. Four values of concentration were used and two temperatures were measured. For pure cyclohexane, the resistance and reactance

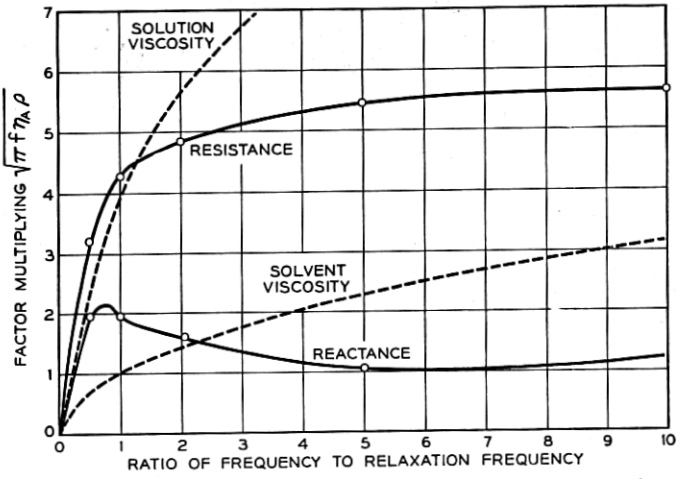

Fig. 9—Resistance and reactance components of a solution having a single relaxation frequency and a solution viscosity 30 times the solvent viscosity.

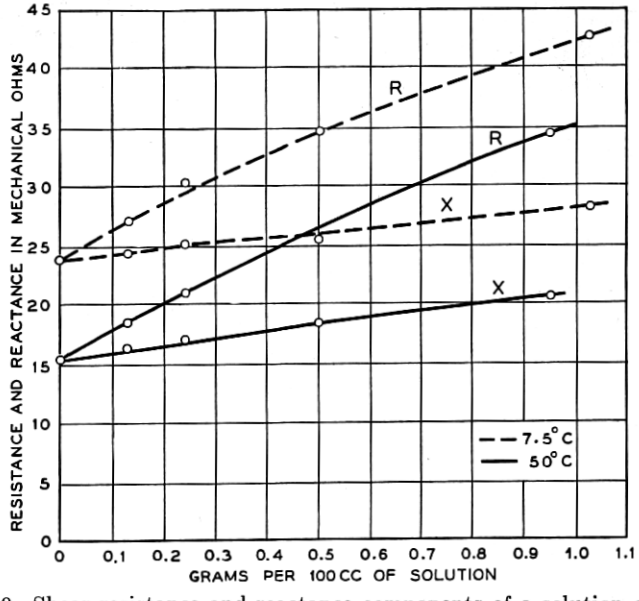

Fig. 10—Shear resistance and reactance components of a solution of polyisobutylene (molecular weight of 3,930,000) in cyclohexane plotted as a function of grams per cc of solution.

components are equal but as the percentage of polyisobutylene is increased, the resistance increases more rapidly than the reactance.

By solving equation (9) for η_A , η_B and μ_B in terms of R and X measured at one frequency and $\eta_A + \eta_B$ the solution viscosity, we find

$$\eta_A = \frac{2RX}{\omega\rho} - \frac{(R^2 - X^2)^2/\omega\rho}{\omega\rho(\eta_A + \eta_B) - 2RX}; \qquad \eta_B = (\eta_A + \eta_B) - \eta_A$$
$$\mu_B = \frac{(R^2 - X^2)\,\omega\eta_B}{\omega\rho(\eta_A + \eta_B) - 2RX} \tag{10}$$

Applying these formulae to the measured results, the curves of Fig. 11 result. The shear elasticity is directly proportional to the concentration, the viscosity η_A is only slightly larger than the solvent viscosity while the main part of the measured viscosity resides in η_B the viscosity associated with chain motion. Fig. 12 shows these three quantities for a one per cent solution measured as a function of temperature. The apparent

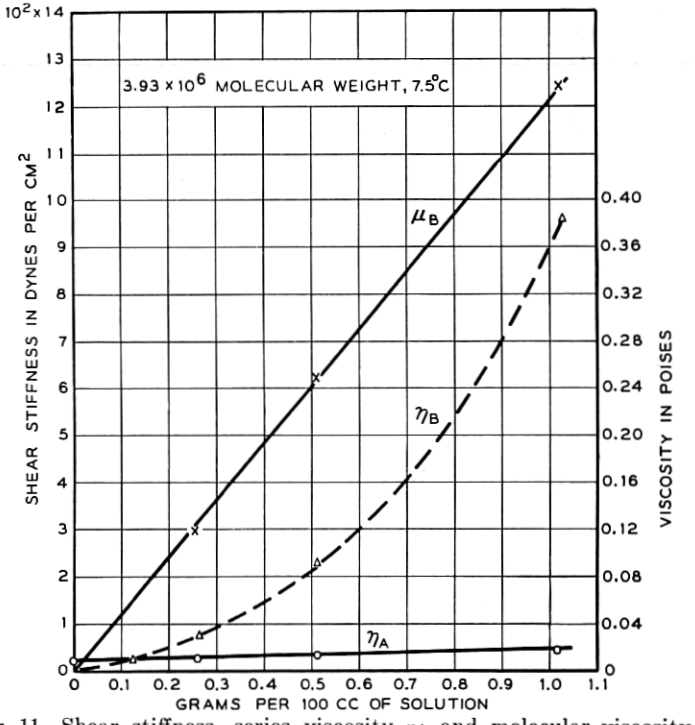

Fig. 11—Shear stiffness, series viscosity η_A and molecular viscosity η_B for polyisobutylene (molecular weight of 3,930,000) in cyclohexane plotted as a function of grams per 100 cc of solution.

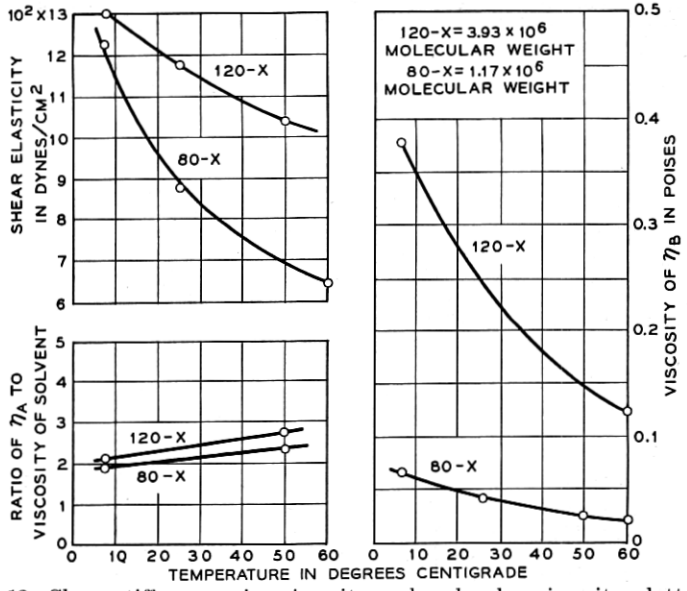

Fig. 12—Shear stiffness, series viscosity and molecular viscosity plotted as a function of temperature for two molecular weight solutions of polyisobutylene in cyclohexane.

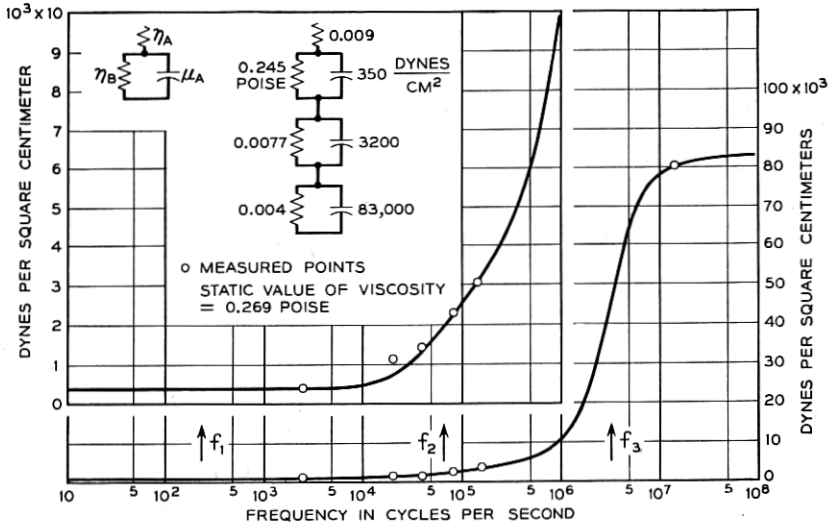

Fig. 13—Shear elasticity for a one per cent solution of polyisobutylene as a function of frequency for 25°C.

stiffness decreases with increase in temperature for a single frequency measurement. However, when measurements were made at 20, 40, 80 and 150 kc it was found that the elasticity was a function of the frequency, which indicates the presence of more than one relaxation and complicates the determination of the temperature relationships. Fig. 13 shows measurements of the shear elasticity over a frequency range from 2.5 kc[10] up to 14 megacycles for 25°C. There is a gradual rise up to about 300 kilocycles after which there is a sharp break to a stiffness of about 90,000 dynes/cm^2 for a 1 per cent solution of the 3,930,000 molecular weight polymer in cyclohexane. If one analyzes the frequency variation of the elasticity he finds that it can be fitted by three relaxation frequencies, one having a frequency of 230 cycles, one around 66,000 cycles and one around 4 megacycles. A possibility exists for a fourth relaxation. The lowest relaxation is thought to be a configurational relaxation of all the elements of the chain. The highest one appears to be a relaxation of the twisting motion of the smallest segment of the chain such as a Kuhn segment. The intermediate relaxation appears to be due to the motion of the ends of the smallest chain segment from one position of entanglement to an adjacent position. This interpretation is based partly on the fact that the associated viscosity of the motion is very similar to that for the relaxation of the twisting motion of the smallest chain segment and partly from data presented in the next section on pure polymer liquids which shows a lower frequency relaxation agreeing in frequency assymptotically with this one, which involves chain motions of approximately 30 to 40 chain elements. Temperature variations of these elastic components show that the lowest relaxation mechanism has a stiffness that increases slightly with temperature in agreement with the kinetic theory of elasticity. The corresponding viscosity (η_2) which comprises most of the viscosity for a solution, when plotted against the reciprocal of the temperature, as shown by Fig. 14, indicates an activation energy of 3.9 kilocalories per mole which is slightly higher than that of the solvent cyclohexane alone, which is about 3.2 kilocalories per mole. This difference of 0.7 kilocalories presumably represents the added energy required to bend the chain in its configurational motion. Measurements with another chain length of 1.18×10^6 molecular weight showed that the stiffness of the lowest (configurational) relaxation decreased from 310 to 160 indicating that the stiffness of this motion is approximately proportional to the square root

[10] The lowest frequency, 2.5 kc, was measured by means of a quartz crystal tuning fork which will be described in another paper. This instrument makes possible the direct measurement of configurational elasticities.

of the molecular weight. The viscosity decreased by a factor of 6.25 and consequently the relaxation frequency increases from 230 to 660 cycles.

The second "entanglement" relaxation has a stiffness of about 3100 dynes/cm^2 for a 1 gram per cc solution of the 3.93×10^6 molecular weight solution and about 2650 dynes/cm^2 for the 1.18×10^6 molecular weight solution. The variation with temperature, if any, is small. The corresponding viscosities η_3 for the two solutions are nearly equal as shown by Fig. 14, and have an activation energy of 4.25 kilocalories per mole. The final high frequency "short segment" relaxation has a high stiffness of 83,000 dynes/cm^2 for a 1 per cent solution of 3.93×10^6 molecular weight. The corresponding viscosities for the two solutions shown by Fig. 14 have nearly identical values and an activation energy of 4.25 kilocalories per mole, i.e. very closely equal to the "entanglement" relaxation viscosity.

These upper two relaxations persist in pure liquid polymers as discussed in the next section, although they are spread out over a small range of relaxation time values. The highest one can be traced in measurements of mechanical properties of solid plastics such as polyethylene and nylon which indicates that these materials should have rubber like

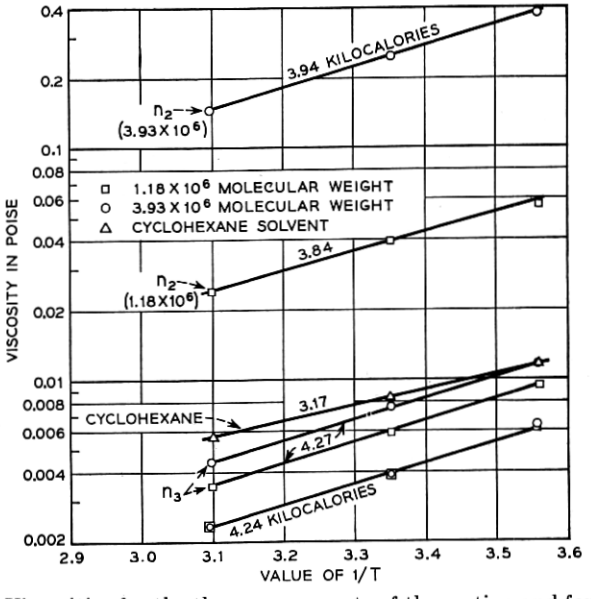

Fig. 14—Viscosities for the three components of the motion and for the solvent plotted against the inverse of the absolute temperature.

TABLE I

Liquid	Average Molecular Weight	Density				Melt Viscosity Poise				No. of Chain Segments
		15°C	25°C	35°C	50°C	15°C	25°C	35°C	50°C	
A	904	0.83	0.826	0.821	0.814	1.10	0.67	0.33	0.16	16.2
B	1,220	0.846	0.842	0.837	0.83	2.64	1.40	0.65	0.297	22.2
C	1,590	0.856	0.849	0.846	0.840	8.4	4.0	2.1	0.87	28.4
D	2,450	0.872	0.866	0.863	0.857	100	38	15.9	4.9	44.0
E	3,520	0.881	0.877	0.872	0.866	580	216	95	30	63.0
F	4,550	0.89	0.886	0.882	0.875	1,960	737	320	98	81.4
G	5,590	0.897	0.892	0.887	0.882	4,600	1,840	740	220	100
H	10,380	0.912	0.908	0.904	0.896	11,500	4,600	2,050	625	186

Measurement at 24 megacycles $\frac{\mu \text{ dynes}}{\text{cm}^2}$; η in poise

Liquid	15°C		25°C		35°C		50°C	
	μ	η	μ	η	μ	η	μ	η
A	0.482×10^9	1.07	0.4×10^9	0.68	0.35×10^9	0.39	0.1×10^9	0.13
B	1.08×10^9	2.64	0.8×10^9	1.39	0.58×10^9	0.7	0.17×10^9	0.293
C	1.65×10^9	5.12	1.2×10^9	2.57	0.885×10^9	1.99	0.27×10^9	0.881
D	2.71×10^9	15.7	2.0×10^9	8.1	1.67×10^9	4.15	0.98×10^9	1.77
E	3.81×10^9	40	3.0×10^9	20	2.17×10^9	10.6	1.2×10^9	4.62
F	5.48×10^9	73	4.22×10^9	38.3	2.8×10^9	20.2	1.6×10^9	8.8
G	5.9×10^9	107	4.78×10^9	51	3.74×10^9	29.5	2.5×10^9	13.2
H	6.9×10^9	119	5.55×10^9	65.8	4.22×10^9	31.5	2.9×10^9	14.8
Measurements at 14 megacycles								
A	0.38×10^9	0.975	0.3×10^9	0.6	0.22×10^9	0.35	0.12×10^9	0.15
B	0.475×10^9	2.53	0.35×10^9	1.4	0.25×10^9	0.74	0.18×10^9	0.53
C	0.68×10^9	3.86	0.61×10^9	3.4	0.3×10^9	1.62	0.25×10^9	0.56
D	2.32×10^9	16.3	1.7×10^9	10	0.94×10^9	4.75	0.39×10^9	1.86
E	3.8×10^9	56.2	2.8×10^9	24.25	2.0×10^9	12.3	0.855×10^9	5.7
F	4.75×10^9	90.4	3.6×10^9	48.3	2.65×10^9	26.6	1.47×10^9	10.8
G	6.03×10^9	136.5	4.6×10^9	81.4	3.24×10^9	39.6	2.0×10^9	15
H	6.64×10^9	160	5.3×10^9	93.5	3.98×10^9	54.2	2.3×10^9	18.5
Measurement at 4.5 megacycles								
A	0.34×10^9	1.18	0.19×10^9	0.64	0.18×10^9	0.34	0.09×10^9	0.17
B	0.55×10^9	2.65	0.21×10^9	1.33	0.2×10^9	0.68	0.1×10^9	0.20
C								
D	1.57×10^9	24	0.96×10^9	11.7	0.72×10^9	5.52	0.34×10^9	2.1
E	2.79×10^9	76	1.9×10^9	37.4	1.43×10^9	16.5	0.9×10^9	5.15
F	3.57×10^9	124	2.5×10^9	61.2	1.86×10^9	31	1.04×10^9	12.8
G	4.4×10^9	176	3.4×10^9	98.5	2.6×10^9	54	1.6×10^9	22.6
H	5.65×10^9	186	4.3×10^9	124	2.8×10^9	76	1.8×10^9	28.8

response to mechanical shocks of very short duration. The lowest frequency configurational relaxation is spread over a wide spectrum of relaxation times in pure liquids.

Measurements[11] of these and other chains in various solvents have also been made and the results are discussed, from a chemical point of view, in a companion paper by W. O. Baker and J. H. Heiss. It is shown that the stiffnesses vary with the polymer chain and the solvent used.

IV. MEASUREMENTS OF PURE LIQUID POLYMERS

A. Shear Wave Measurements in Liquid Polymers

Similar shear wave measurements have been made for pure polyisobutylene liquids of molecular weights from 904 to 10,380 (i.e. from 16 chain elements to 186 chain elements), by the techniques described in Section II. Some of these results have been discussed in reference (8) but the much more comprehensive measurements made since require some revisions of the original conclusions.

The easiest data to interpret are the high-frequency data obtained by the shear wave reflectance method. The data of Table I give measurements of 8 liquids varying in average molecular weight from 900 to 10,380, at three frequencies and four temperatures. If we plot for example the Maxwell shear stiffness and viscosity for the three frequencies and for 25°C as a function of the number of chain elements (here a chain element is taken as two adjacent carbon atoms one of which has two methyl groups attached and the other two hydrogens) the 4.5-mc measurements are shown by the triangles of Fig. 15. The 14 megacycle measurements are shown by the circles and the 24-mc measurements by the squares.

An attempt was made to fit these measurements with a two relaxation mechanism shown by the figure with two stiffnesses which are taken to be independent of the molecular weight and equal respectively to 1.2×10^8 dynes/cm^2 and 6×10^9 dynes/cm^2. The best fit is obtained by taking the two viscosities η_1 and η_2 equal and these are adjusted for the different molecular weights in such a manner as to best fit the experimental curve. A fair agreement is obtained except for the range from 60 to 90 chain elements where the two relaxation model gives too rapid an increase of stiffness with increase in the number of chain elements and at the high molecular weight viscosity range where the viscosity shows a dispersion in values but the model does not. The sum of the two vis-

[11] These results on the mechanical impedance of long chain molecules in solvents have been presented at the XIIth International Congress of Pure and Applied Chemistry by W. O. Baker, W. P. Mason and J. H. Heiss, Sept. 13, 1951.

cosities η_1 and η_2 assumed as a function of molecular weight is shown by Fig. 16. The log of the viscosity starts proportional to the molecular weight but above a molecular weight of 2,400 the increase is very slow and becomes asymptotic to a value of 240 poises. An equation which fits the increase in viscosity with molecular weight is

$$\eta_D = Ke^{11.8 \tanh Z/2370}$$

where Z is the molecular weight. The solid line shows a plot of this curve and the circles are the assumed values to obtain a best fit to the meas-

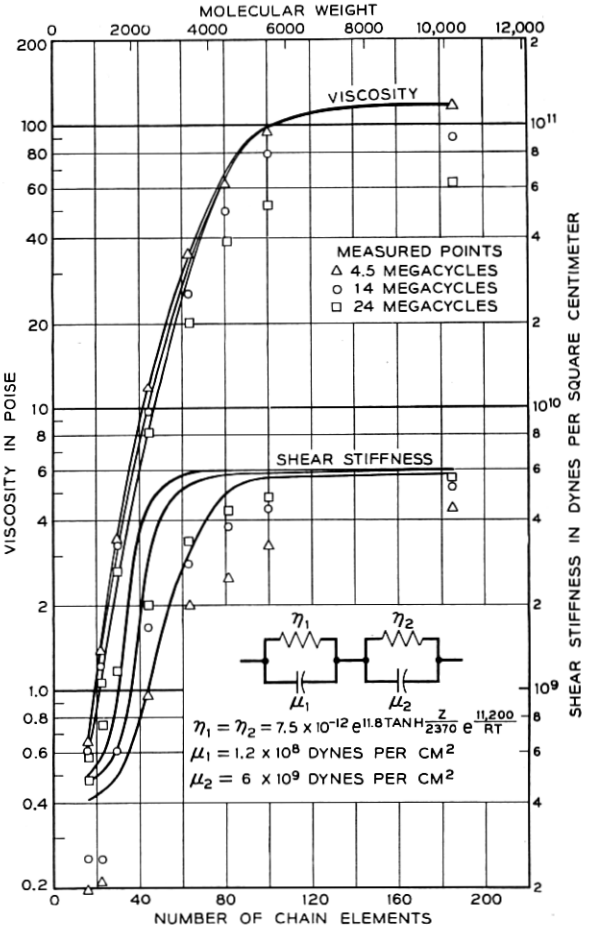

Fig. 15—Measured values of high frequency shear viscosity and elasticity for 25°C and three frequencies plotted against molecular weight. Solid lines are best fit obtained by a two relaxation mechanism having the element values shown by the figure.

ured values. This equation indicates that when $Z = 2{,}370$ or 43 chain elements the viscosity increases only a small amount more by a chain articulation effect and hence in this high frequency range we are dealing with a chain length of about 40 elements or 80 carbon atoms. This is checked also by a comparison of the static and dynamic viscosity. The total dynamic viscosity due to the two relaxation mechanisms compared to the static viscosity does not differ markedly until the number of chain elements is more than 40. Above this value other motions than that of the shortest chain segment can take place and can add to the dynamic viscosity. The static viscosity fits an equation of the same sort, but the indicated chain length for the viscous motion is about $\frac{5}{3}$ times that of the shortest segment.

When a similar process is carried out over the temperature range the equations of Fig. 16 are obtained. The static viscosity has an activation energy of 16 kilocalories per mole, while the dynamic viscosity has an activation energy of about 11.2 kilocalories per mole.

The relaxation frequencies for the two components are plotted as a function of the number of chain segments by the solid lines of Fig. 17.

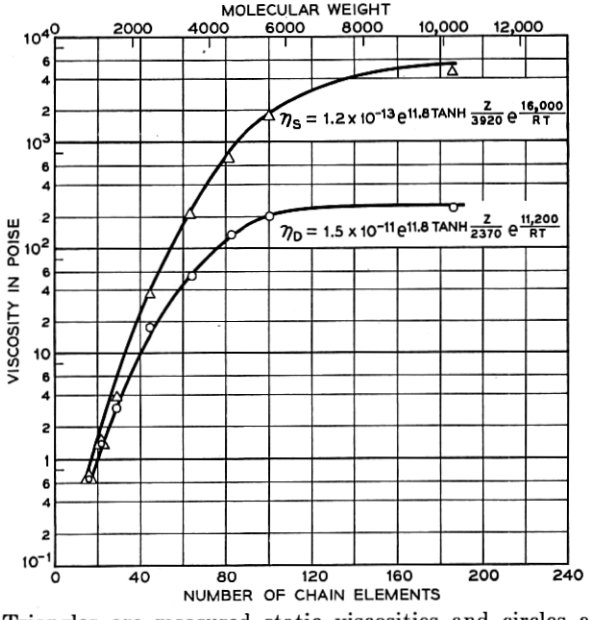

Fig. 16—Triangles are measured static viscosities and circles are dynamic viscosities plotted as a function of molecular weight. Solid lines are a plot of the equations given for static and dynamic viscosities.

For long chain segments the values become asymptotic to 8×10^6 cycles and 160,000 cycles which are not far from the two highest relaxation frequencies obtained from the solution measurements of Section III. Hence it appears likely that these relaxations are due to the "entanglement" motion and the twisting motion of the shortest chain segment. The increased activation energy is due to the fact that more energy has to be applied to the chain segment to break it loose from its equilibrium position when it is surrounded by adjacent polyisobutylene molecules than when it is surrounded by cyclohexane molecules. The stiffness of the chain is due more to the slope of the potential well than to any intrinsic chain stiffness as is shown by Fig. 18, which shows the two stiffnesses as a function of temperature. These values are obtained by fitting the 15°, 35° and 50° data in a similar manner to that used for the 25°

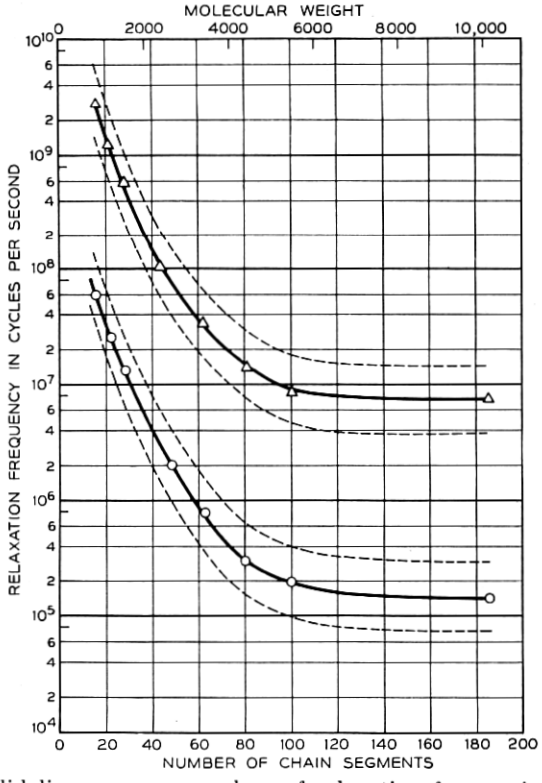

Fig. 17—Solid lines are mean values of relaxation frequencies for the two mechanisms plotted against molecular weight. Dotted lines indicate limits of regions assumed to obtain a better fit to the measured values.

data, and the activation energy of 11.2 kilocalories per mole is obtained in a similar manner.

Due to the closeness of the surrounding polyisobutylene molecules, one would expect that the relaxation frequencies would not have discrete values but would be spread about the center value in some sort of a Gaussian distribution. If we approximate this by representing each region by two relaxations, one-half, and the other twice the frequency of the mean value, as shown by the dotted lines of Fig. 17, the agreement with the measured values of Fig. 15 is considerably better as shown by Fig. 19. A wider distribution yet is indicated.

For molecular weights greater than 2,000 the shortest chain segment viscosity begins to diverge from the static viscosity indicating that there are other relaxations for these longer chains. Some data for the three longest chain polymers, F, G and H have been obtained by the torsional rod method and the results are given in Table II. These data are plotted on Fig. 20 as a ratio of dynamic to static viscosity plotted

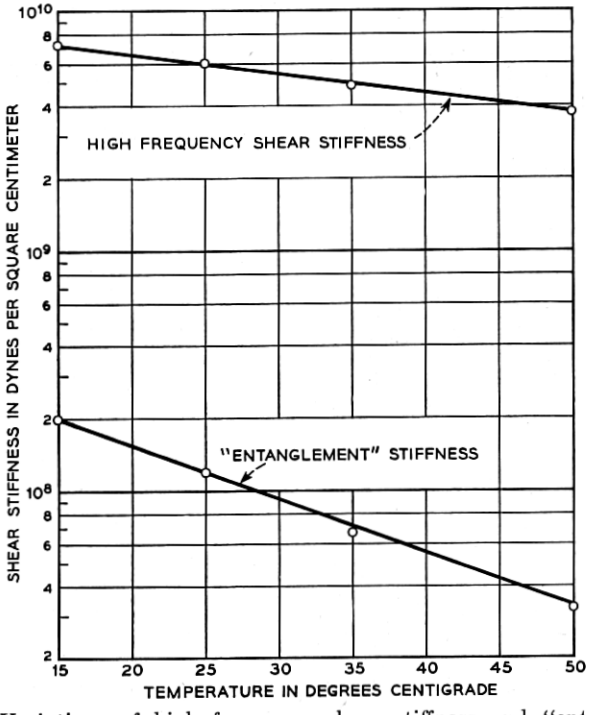

Fig. 18—Variations of high frequency shear stiffness and "entanglement" stiffness plotted as a function of the temperature.

against the frequency times the static viscosity. All the viscosity data can be represented within the experimental error by a single curve, but the stiffness curves appear to require different curves for different temperatures. On analyzing the data in terms of a distribution of relaxation frequencies, a single curve for all temperatures could be obtained if the stiffness of each mechanism were independent of the temperature and the relaxation frequency were inversely proportional to the static viscosity, i.e., had an activation energy variation equal to that for the static viscosity for each relaxation mechanism. This condition holds

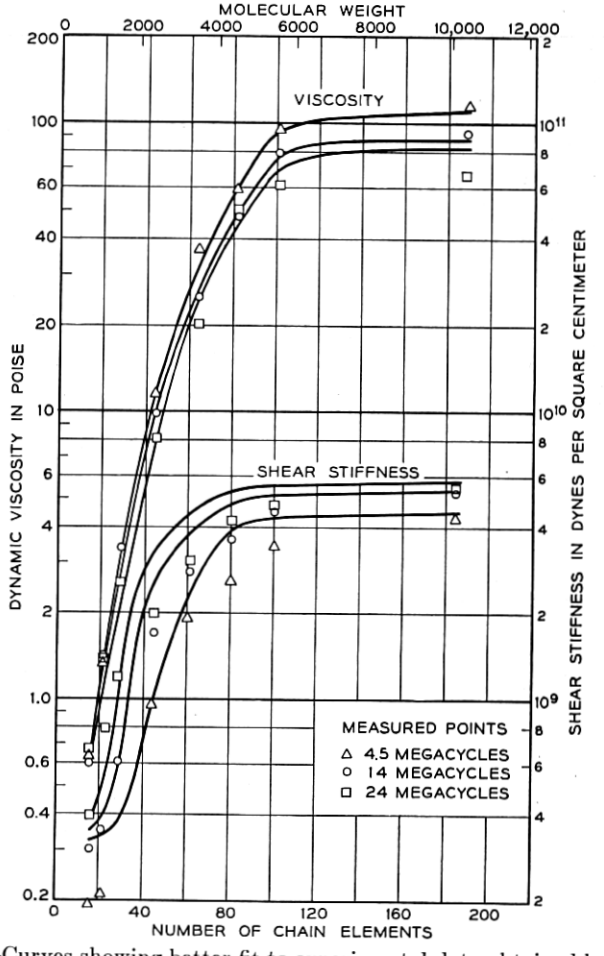

Fig. 19—Curves showing better fit to experimental data obtained by assuming the relaxation regions shown by Fig. 17.

TABLE II

Measurement for Polymer F—Molecular weight = 4550

Frequency Kilocycles	15°C		25°C		35°C		45°C		55°C		65°C	
	μ	η	μ	η	μ	η	μ	η	μ	η	μ	η
25	2.9×10^8	600	1.45×10^8	270	0.78×10^8	145	0.44×10^8	77	0.26×10^8	43	0.17×10^8	24
40	3.8×10^8	550	1.7×10^8	250	0.86×10^8	125	0.47×10^8	66	0.28×10^8	38	0.20×10^8	22
52	4.0×10^8	470	1.9×10^8	220	0.78×10^8	110	0.54×10^8	59	0.33×10^8	34	0.21×10^8	20
140	5.8×10^8	380	3.0×10^8	180	1.5×10^8	91	0.71×10^8	48	0.44×10^8	26	0.28×10^8	17

Polymer G—Molecular weight = 5590

Frequency Kilocycles	24.5°C		65°C	
	μ	η	μ	η
27.5	2.0×10^8	510	1.9×10^7	38.4
40.96	2.95×10^8	480		
54.23	3.60×10^8	456	2.93×10^7	36.1

Polymer H—Molecular weight = 10,380

Frequency Kilocycles	55°C		67°C	
	μ	η	μ	η
32.2	3.9×10^7	150	2.9×10^7	94
40.5	4.8×10^7	137	3.5×10^7	86
47.0	5.3×10^7	126	3.9×10^7	79

quite well for frequencies much lower than the relaxation frequencies of the smallest chain segment, but as the frequency approaches these relaxation frequencies, the stiffness of these polymers increases as the temperature decreases.

A fair approximation to these measured values is obtained by assuming one more "configurational" relaxation frequency in addition to the two smallest segment relaxations discussed previously. Fig. 21 shows calculations of the ratio of dynamic to static viscosity and the shear stiffness for 65°C and 25°C. The lowest relaxation frequency is assumed to have a stiffness of 6.3×10^6 dynes/cm^2 and a viscosity of 20 poises at 65°C. For 25°C the stiffness of 2×10^7 dynes/cm^2 is assumed and an activation energy of 17.3 kilocalories gives the component a viscosity of 607 poises at 25°C, and a relaxation frequency of 5,250 cycles. The average value of 16 kilocalories for the static viscosity is a result of the sum of the variation due to the two components. Although the agreement can be improved by assuming distributions of relaxation frequencies centered around these three primary frequencies, there does not seem to be much doubt of the existence of these primary relaxation

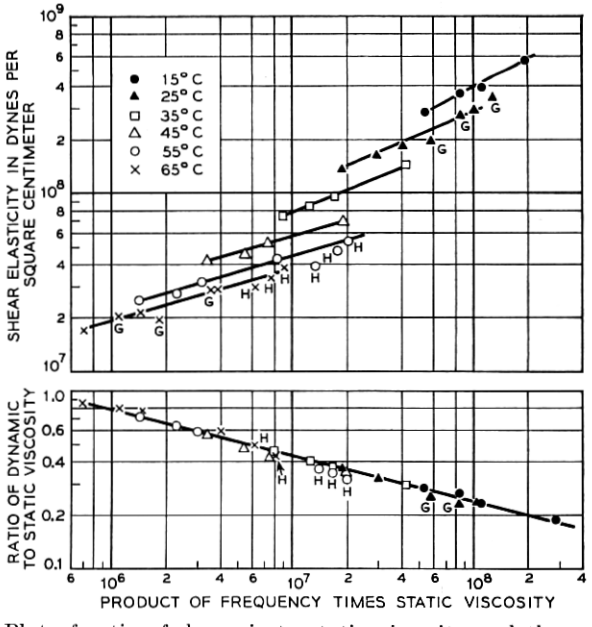

Fig. 20—Plot of ratio of dynamic to static viscosity and the corresponding intermediate frequency shear stiffnesses as a function of temperature and product of frequency times static viscosity.

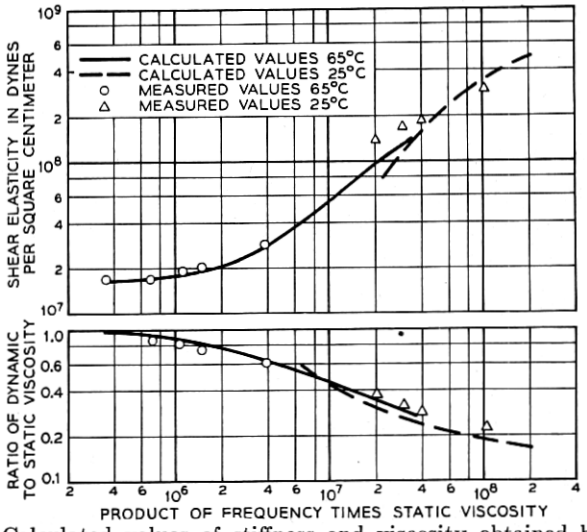

Fig. 21—Calculated values of stiffness and viscosity obtained by adding a single "configurational" relaxation frequency to the two short chain relaxations obtained from high frequency measurements.

mechanisms which show up as discrete relaxations in long chain molecules in solution.

Some measurements have also been made to determine the effect of chemical substitutions in the polymer chains. In a previous paper,* the high frequency properties of poly-α-methyl styrene were discussed. This material has the polyisobutylene chain but with one methyl replaced by a phenyl so that its chain becomes

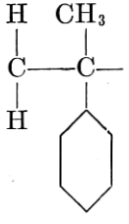

For low molecular weights this material is liquid. The shear stiffness of this liquid is somewhat higher than for polyisobutylene but has about the same change with temperature. The variation of the high-frequency viscosity, however, is much larger for poly-α-methyl styrene than for polyisobutylene, and corresponds to an activation energy of 23.6 kilocalories. The relaxation region for the shortest chain motion is much

* See footnote on page 132.

narrower than in polyisobutylene, which correlates with the smaller steric hindrance.

Measurements have also been made in the 70-kc to 140-kc range for two non polar liquids, polybutadiene and polypropylene and one polar liquid, polypropylene sebacate. The first two have the formulae

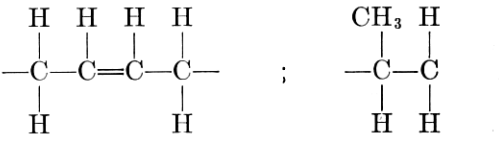

polybutadiene ; polypropylene

while the polar liquid, polypropylene sebacate, has the formulae

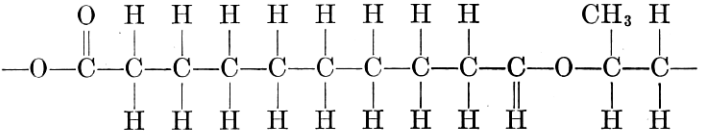

TABLE III

Temp. °C	Density ρ	Poise Static Viscosity η_s	76.5 Kc Measurements				142.6 Kc Measurements			
			Maxwell		η_D/η_s	$f\eta_s$	Maxwell		η_D/η_s	$f\eta_s$
			η_D poise	μ dynes/cm²			η_D poise	μ dynes/cm²		
Polybutadiene										
10	0.877	740	25.5	7.83×10^6	0.0355	5.66×10^7	14.65	9.96×10^6	0.0196	10.55×10^7
20	0.873	450	21.1	6.38×10^6	0.0469	3.44×10^7	13.45	7.91×10^6	0.0299	6.41×10^7
30	0.869	288	17.45	5.3×10^6	0.0605	2.21×10^7	12.4	6.67×10^6	0.043	4.11×10^7
40	0.865	189	15.3	4.67×10^6	0.081	1.44×10^7	11.05	5.96×10^6	0.0583	2.69×10^7
50	0.861	128	11.9	3.92×10^6	0.093	0.98×10^7	9.16	5.21×10^6	0.0715	1.82×10^7
60	0.857	88	9.85	3.55×10^6	0.112	0.67×10^7	7.51	4.54×10^6	0.0855	1.25×10^7
Polypropylene										
			76.5 Kc Measurements				142.5 Kc Measurements			
45	0.849	30,000	380	3.56×10^8	0.01265	2.3×10^9	354.5	6.69×10^8	0.0118	4.26×10^9
55	0.842	10,900	160.2	1.4×10^8	0.0153	0.832×10^9	167	3.18×10^8	0.0153	1.55×10^9
65	0.836	4,200	89.8	0.786×10^8	0.0214	0.321×10^9	79.1	1.46×10^8	0.0188	0.6×10^9
75	0.830	1,600	50.8	0.444×10^8	0.0318	0.128×10^9	46.6	0.998×10^8	0.0292	0.23×10^9
85	0.824	700	31.2	0.264×10^8	0.0446	0.053×10^9	28.4	0.51×10^8	0.0405	0.10×10^9
Polypropylene Sebacate										
			77.1 Kc Measurements				141.5 Kc Measurements			
5	1.076	9,200	95.2	4.88×10^7	0.0103	7.1×10^8	74.6	7.45×10^7	0.0081	1.3×10^9
15	1.068	4,200	67.6	2.94×10^7	0.0161	3.24×10^8	54.9	4.28×10^7	0.0131	0.595×10^9
25	1.060	2,060	51.4	2.01×10^7	0.0249	1.6×10^8	41.3	2.82×10^7	0.02	0.292×10^9
35	1.051	1,050	43.1	1.54×10^7	0.0411	0.81×10^8	33.2	1.97×10^7	0.0316	0.148×10^9
45	1.042	580	38.8	1.24×10^7	0.0669	0.45×10^8	26.9	1.69×10^7	0.0464	0.082×10^9
55	1.034	320	32.8	1.01×10^7	0.1023	0.25×10^8	24.2	1.34×10^7	0.0756	0.045×10^9
65	1.026	183	26.8	0.88×10^7	0.147	0.14×10^8	22.9	1.25×10^7	0.125	0.026×10^9

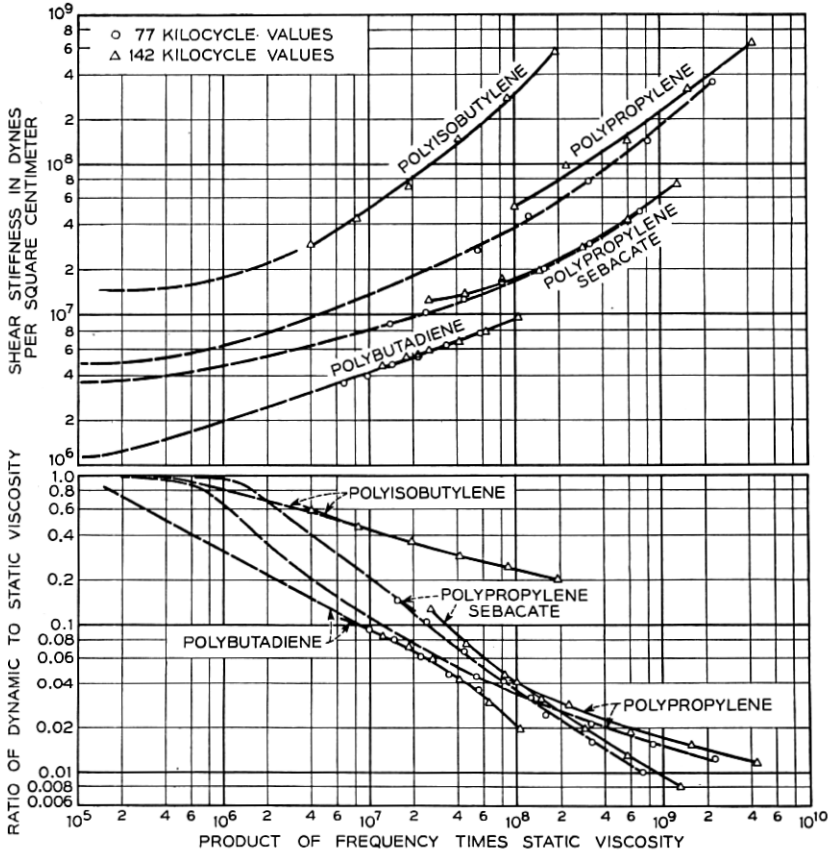

Fig. 22—Ratio of dynamic to static viscosity and the shear stiffness for four polymer liquids plotted against product of frequency and static viscosity.

the 4.8 kilocalories for polyisobutylene. This presumably indicates that there is more of a difference between the viscosity flow segment and the shortest chain segment in these materials than in polyisobutylene. Since no measurements are available over a range of molecular weights, no direct evidence has been obtained for the various chain lengths.

B. Longitudinal Wave Measurements in Liquid Polymers

Since the increase in shear elasticity for the highest relaxation frequency is so large, it should also appear in longitudinal wave measurements. Fig. 23 shows a calculation for the 5590 molecular weight liquid of the longitudinal velocity assuming that the Lamé λ elastic constant is independent of frequency and that all the variation occurs in the shear

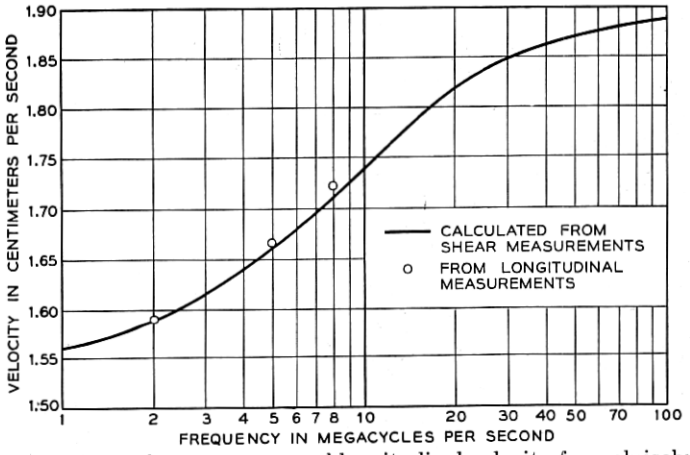

Fig. 23—Relation between measured longitudinal velocity for polyisobutylene of molecular weight 5590 and that calculated from shear stiffness measurements assuming the Lamé λ elastic constant is independent of frequency.

constant as determined by the shear measurements. The points are velocities measured for longitudinal waves and as can be seen, the measurements agree closely with the calculated values. A slightly better agreement would be obtained if λ increased by a small amount as the frequency increased. As discussed in the next section there is some experimental evidence for an increase in λ in nylon 6-6 and in polyethylene.

The question also arises as to how much of the attenuation is due to shear mechanisms and how much due to pure compressional effects. From longitudinal velocity and attenuation measurements at 30°C for the polymers E, F and G of Table I, the values of $\lambda + 2\mu$ and $\chi + 2\eta$ can be determined and are shown by Table IV. The values of μ and η can be obtained from Table I by interpolation and are given in columns

TABLE IV

Polymer	$\lambda + 2\mu$ dynes/cm²	$\chi + 2\eta$ poise	μ dynes/cm²	η poise	λ dynes/cm²	χ
			5 megacycles			
E	1.92×10^{10}	62	0.17×10^{10}	26	1.60×10^{10}	10
F	2.26	107	0.23×10^{10}	46	1.70×10^{10}	15
G	2.38	170	0.31×10^{10}	75	1.76×10^{10}	20
			8 megacycles			
E	2.01×10^{10}	50	0.20×10^{10}	22	1.61×10^{10}	6
F	2.26	93	0.27×10^{10}	41	1.72×10^{10}	11
G	2.56	155	0.34×10^{10}	69	1.88×10^{10}	17

4 and 5. Columns 6 and 7 show the values of λ and χ, the compressional components. A definite longitudinal compressional viscosity is indicated which however is somewhat smaller than the shear viscosity η.

V. MEASUREMENTS FOR SOLID POLYMERS

Recently two new methods have been devised for accurately measuring the properties of solid plastics in the ultrasonic frequency range

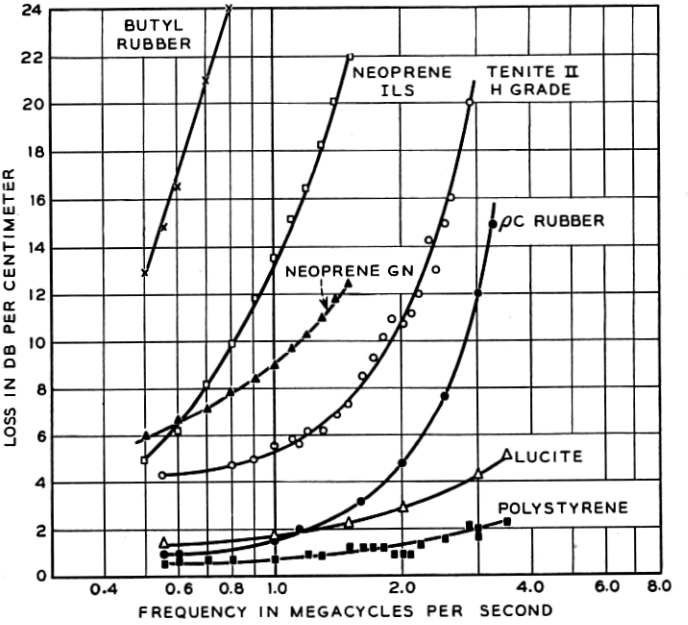

Fig. 24—Normal loss in db per centimeter measured as a function of frequency for several rubbers and plastics.

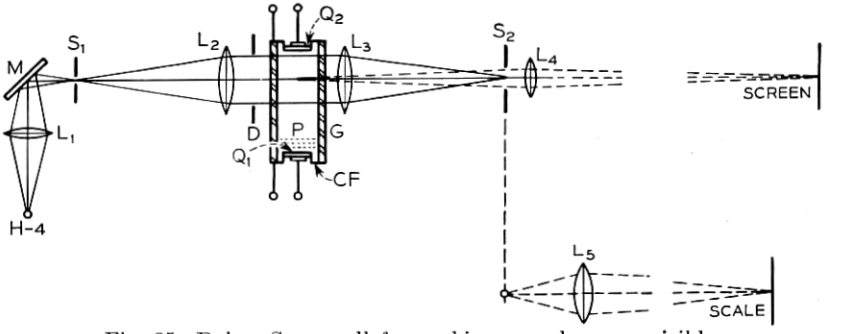

Fig. 25—Debye-Sears cell for making sound waves visible.

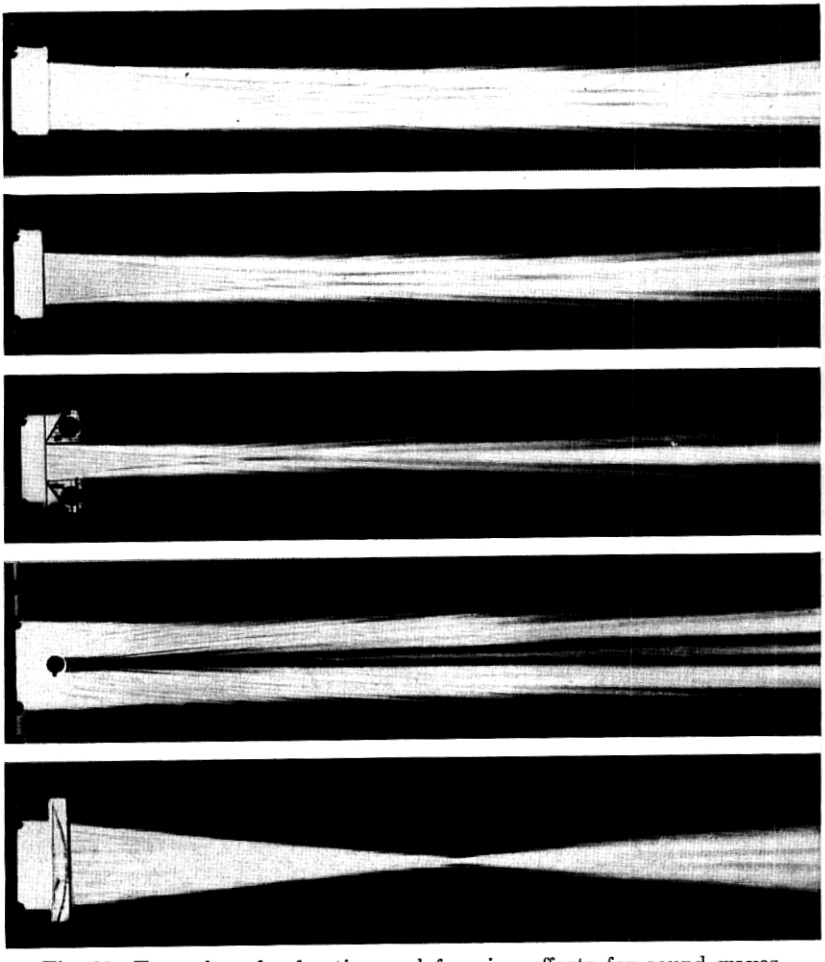

Fig. 26—Examples of refraction and focusing effects for sound waves.

and these have shown relaxations in such plastics as polyethylene and nylon 6-6. The simplest method for measuring one of the properties for longitudinal waves, i.e., the attenuation, is to measure the change in loss between two transducers in a liquid such as water, caused by inserting a sheet of the material. This process, used during the last war, results in the losses in db per centimeter for several rubbers and plastics, shown by Fig. 24. Indications of relaxation mechanisms are given by the rubbers and the plastic tenite II which is a cellulose acetate butyrate. The first fairly accurate method for measuring longitudinal sound

velocities[12] in plastics was the method of observing the focusing effect of a cylindrical lens made of the plastic. Sound waves can be made visible by the Debye-Sears technique of using a sound wave as a phase diffraction grating. Here light from a slit S_1 is made parallel by the lens L_2 and passes through the cell parallel to the wave fronts of the sound waves as shown by Fig. 25. The compressed parts of the medium retard the light waves more than the rarefied parts do and hence the medium acts as a phase diffraction grating. If a second slit S_2 is used which is small enough to pass only the zero order, a light valve action is obtained which modulates the light according to the sound wave intensity. If now the lens L_5 is used which focuses on the median plane of the tank, a picture of the sound beam is obtained as shown on Fig. 26. The bottom figure shows the focusing effect of a plastic and from the focal distance d and the radius of curvature r of the lense, one can calculate the velocity in a plastic compared to the velocity in the water by the formula

$$v_p = v_w \Big/ \left(1 - \frac{r}{d}\right) \tag{11}$$

This method gives velocities good to from 2 to 5 per cent depending on the attenuation in the lens.

G. W. Willard[13] has devised recently a more accurate method for measuring sound velocities as shown schematically by Fig. 27. Here a plastic to be measured is placed half way across the sound beam in the liquid and light is sent along the wave front occurring in both the plastic and the liquid. If the waves are in phase the retardation in the two light gratings, corresponding to sound propagation in both media, add up and for a slit selecting the zero order the darkest pattern occurs on the photographic plate. If the two waves are just out of phase, the retardation is reversed in the two media and the lightest part occurs. With this relation it can be shown[13] that the spacing d of light and dark lines

[12] W. P. Mason, *Piezoelectric Crystals and Their Application to Ultrasonics*, D. Van Nostrand, 1950, p. 404. It was used in this country by G. W. Willard as early as 1940. It was also used in Germany by J. Schaefer "Eine Neue Method Zur Messung der Ultraschallwellen in Festkorpern." Diss Strassburg, 1942. By making the front surface part of a cylinder, Schaefer also measured the shear velocity in a solid.

[13] G. W. Willard, *J. Acous. Soc. Am.*, **23**, Jan. 1951, pp. 83–94. The origin of this multiple path interference method goes back to the work of R. Bär (Helvetia Physica Physica Acta Bd 13 page 61 (1940)) who attached a piezoelectric crystal to a bar with a 45° end section and set up transverse and longitudinal waves, in the bar. These waves produced longitudinal waves in a surrounding liquid and by observing the interference pattern between them, the longitudinal and shear constants could be determined for an isotropic medium. Willard's method as described above is much more direct and is capable of higher accuracies.

is related to the wavelength in the liquid λ_ℓ and the wavelength in the solid λ_s, by

$$\frac{1}{d} = \frac{1}{\lambda_\ell} - \frac{1}{\lambda_s} \tag{12}$$

This corresponds to a velocity in the solid compared to a velocity in the liquid given by

$$v_s = \frac{v_\ell}{1 - v_\ell/fd} \tag{13}$$

where f is the frequency. Fig. 28 shows a photograph of a series of lines in a transparent plastic and a transparent plastic in the form of a wedge. It is seen that beyond the edge of the plastic there is a dark interference band for each one in the transparent plastic. This phenomenon is caused by the refraction of the sound wave that has traversed the plastic and the dark lines are lines of equal phase of the two waves in the liquid. The angle of the dark lines is half the refraction angle. Hence the velocity can also be determined by counting the number of dark bands in the liquid beyond the plastic. This makes it possible to measure the veloci-

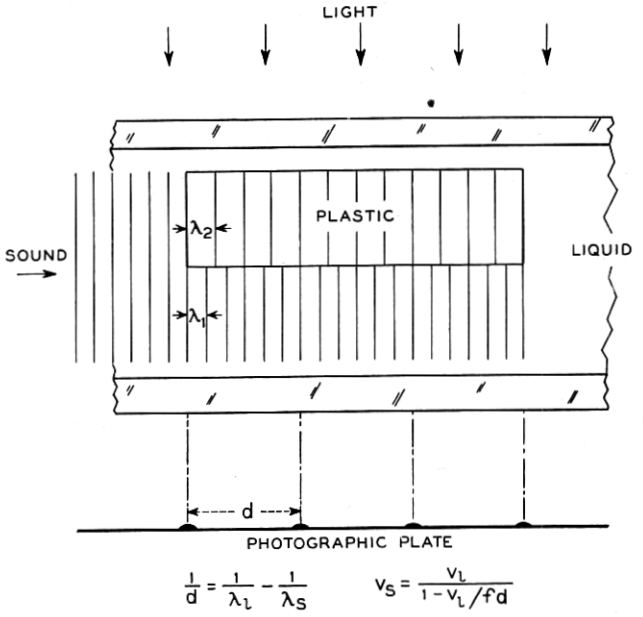

Fig. 27—Optical method for measuring sound velocities of plastics by comparing their velocity with that of a liquid such as water.

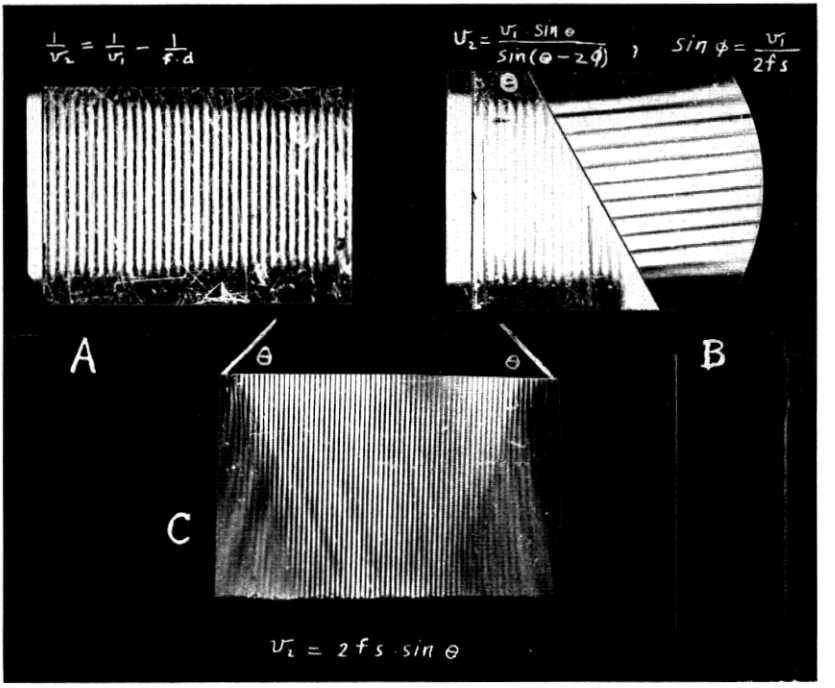

Fig. 28—Photographs of interference patterns from sound waves in liquids and plastics.

ties in opaque plastics. The accuracy of the method is better than 1 per cent if the attenuation is low enough to give a number of interference lines. For plastics of high internal loss, the method becomes somewhat inaccurate.

Typical measurements using this system are shown in Table V. Small changes in chemical composition and plasticizer content are shown up as can be seen from the table. Of particular interest is the difference between nylon 6-6 and polyethylene. Chemically as shown by Fig. 29, the two are identical except for the dipoles occurring for every 6 units of the ethylene chain. These dipoles have the effect of bonding adjacent layers together and result in a higher shearing modulus.

By attaching shear vibrating crystals to a right angled prism, as shown by the lower part of Fig. 28, with the direction of motion of the crystals parallel to the transmitting face, and setting up shear standing waves between the two crystals, the shear properties of the plastic can be measured. Longitudinal waves are generated in the liquid which interfere with one another and cause dark bands perpendicular to the plastic

TABLE V

Measured longitudinal velocity and attenuation at 25°C and 2.5 mc. Longitudinal attenuation in DB/cm at 25°C and 2.5 mc except as noted.

Material	Long velocity $\times 10^{-5}$ cm/sec	Shear velocity 10^{-5} cm/sec	A DB/cm	Density
Dural, 17 ST	6.5	3.12	—	2.7
Brass, half hard	4.7	2.11	—	—
Polystyrene	2.35	1.12	2	1.05
Plexiglas	2.68		5	1.18
Tenite II, (cellulose acetate butyrate), 2% plasticizer	2.08		9	1.23
Tenite II, 13% plasticizer	2.02		10	1.21
Polyvinal formal	2.68		10	1.24
Polyvinlidene chloride	2.4		18	1.71
Poly N-butyl methacrylate	1.96		5	1.05
Poly I-butyl methacrylate	2.08		6	1.05
Neoprene	1.51		20	.99
Polyethylene	2.0		4.7 $F^{1.11}$	.90
Nylon 6-6 (3–30 megacycles)	2.68		1.0 $F^{1.5}$	1.11
Nylon 6-10 (3–30 megacycles)	2.56		1.0 $F^{1.5}$	1.11

surface. By determining the spacing of these lines the velocity of the shear waves can be determined.

Another method has also been developed which is more applicable for high loss materials. This is a pulsing method and is a modification of the method proposed by one of the authors for measuring the properties of small crystal specimens.[14] Here longitudinal or shear crystals are soldered to the fused quartz rod as shown by Fig. 30 and a sample to be measured is placed between these by means of a liquid such as polyisobutylene which has a high shear elasticity. If the specimen has a small attenuation, this can be measured by taking the difference in the amplitude of successive reflections. If the specimen has a high loss, this does not work and another method has been used which consists in sending a pulse from both crystals.[15] One crystal is then used to receive and it receives the wave sent through the sample and the wave reflected from the fused quartz-sample interface. By adjusting the amplitude until these two are equal and the frequency or phase of one channel until the waves cancel, a ratio of amplitudes and a frequency of half wavelength are accurately determined. From these the velocity and attenuation can be calculated.

This method has been applied to measuring the longitudinal and shear velocities of polyethylene and 6-6 nylon. The polyethylene was of "equilibrium" crystallinity and average molecular weight corresponding to

[14] H. J. McSkimin, "Ultrasonic Measurement Techniques Applicable to Small Solid Specimens," *J. Acoust. Soc. Am.*, **22**, No. 4, July 1950, pp. 413–418.

[15] H. J. McSkimin, *J. Acoust. Soc. Am.*, **23**, No. 4, pp. 429–435.

an intrinsic viscosity in xylene of [n] = 0.89 at 85°C. Fig. 31 shows the longitudinal velocity of polyethylene plotted as a function of frequency and temperature. The velocity rises with frequency and a dispersion is indicated. This is confirmed by the attenuation per wavelength curve for two different frequencies plotted as a function of temperature, Fig. 32. A definite dispersion is seen to occur with an activation energy of about 12 ± 2 kilocalories per mole. This could occur in either the λ constant or the shearing constants μ, but the data of Figs. 33 and 34 show definitely that it occurs in the shear component. Fig. 33 shows the shear velocity for four temperatures plotted as a function of frequency. This can be fitted for 30°C with a single relaxation mechanism having a relaxation frequency of 8 megacycles. To agree with the measured attenuation and velocity, there has to be a spreading of the single relaxation over a range as also occurs in liquids. The indicated shear stiffness below this relaxation frequency is 2.6×10^9 dynes/cm^2. Some

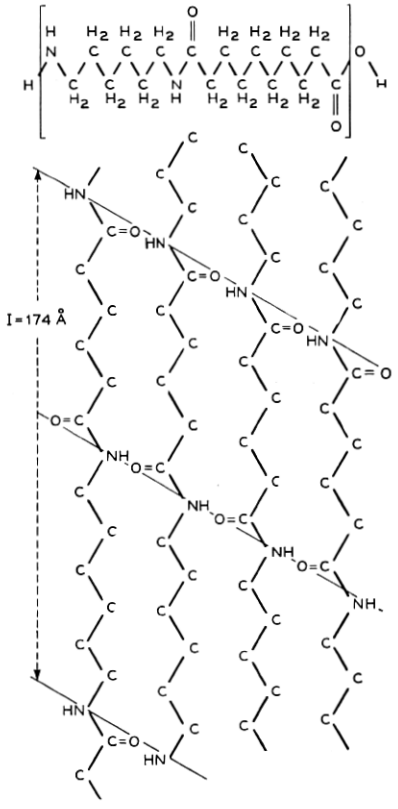

Fig. 29—Spatial structure of nylon 6-6.

data on the zero frequency shear modulus is obtained from the Young's modulus for a static pull which is from 30,000 to 50,000 pounds/square inch. Since the Young's modulus is three times the shearing modulus, the zero frequency shearing modulus should not exceed 1.1×10^9 dynes/cm^2. Hence one may expect that other relaxations will occur at lower frequencies.

Fig. 34 shows the attenuation per wavelength for shear waves. The solid line for 30°C represents the calculated attenuation per wavelength for the model assumed. If all the dissipation were due to shear mechanisms, the calculated attenuations would occur as shown by the 30°C

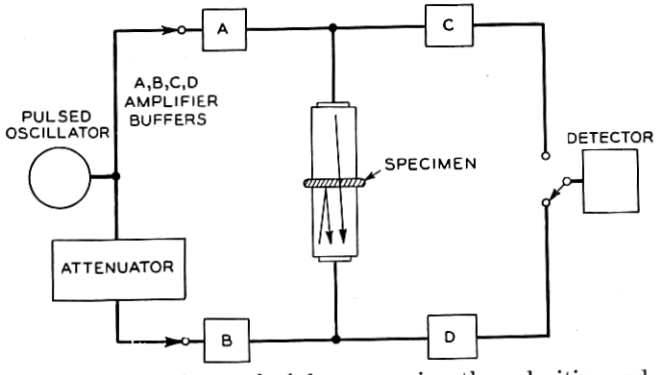

Fig. 30—Ultrasonic pulse method for measuring the velocities and attenuations of highly attenuating plastics.

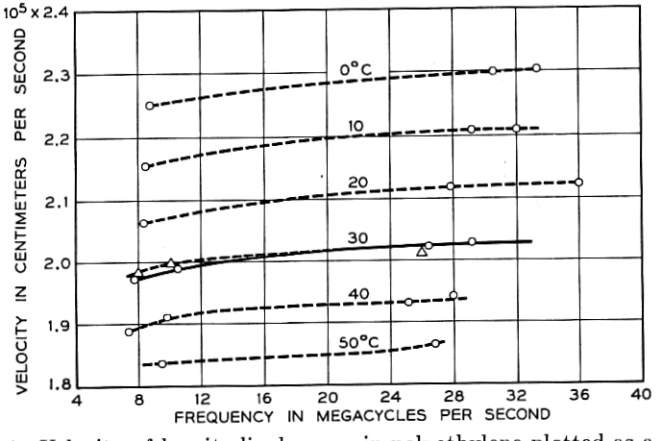

Fig. 31—Velocity of longitudinal waves in polyethylene plotted as a function of temperature and frequency.

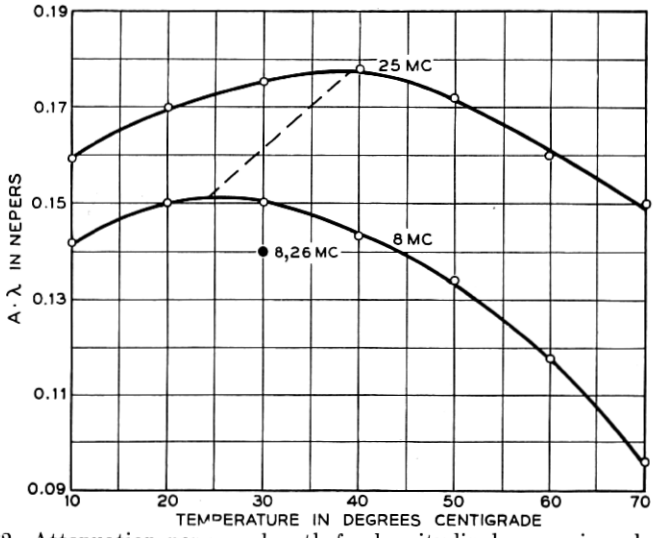

Fig. 32—Attenuation per wavelength for longitudinal waves in polyethylene plotted as a function of temperature and frequency.

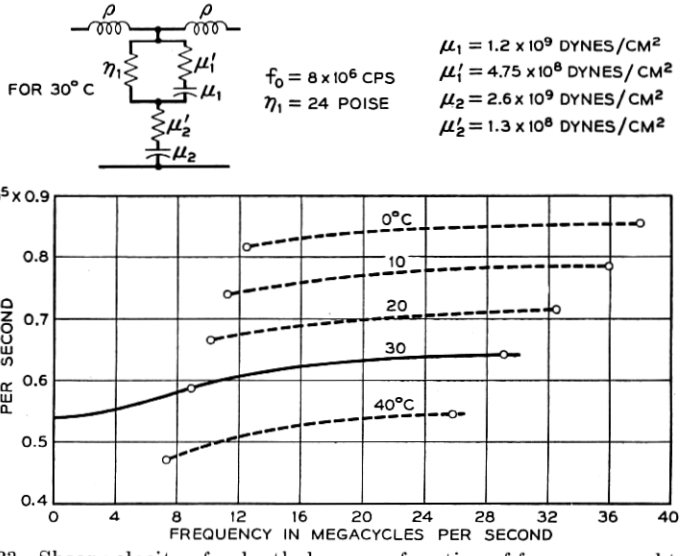

Fig. 33—Shear velocity of polyethylene as a function of frequency and temperature. Equivalent circuit shows elements necessary to account for the velocity and attenuation changes at 30°C.

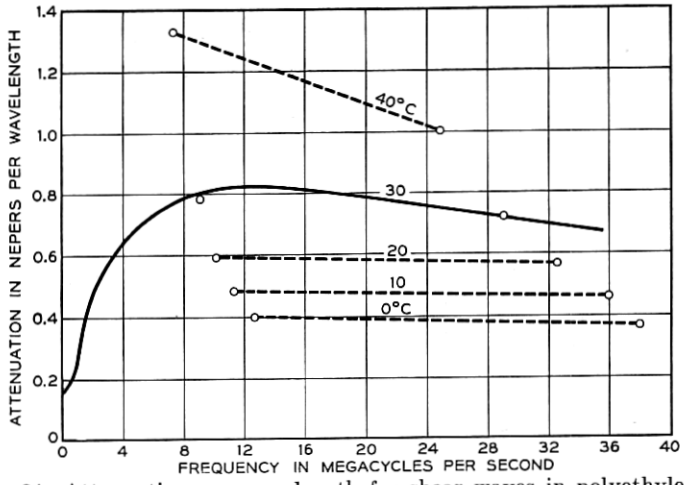

Fig. 34—Attenuation per wavelength for shear waves in polyethylene.

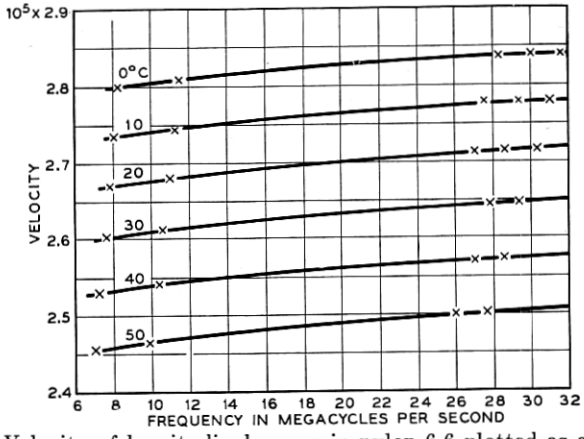

Fig. 35—Velocity of longitudinal waves in nylon 6-6 plotted as a function of temperature and frequency.

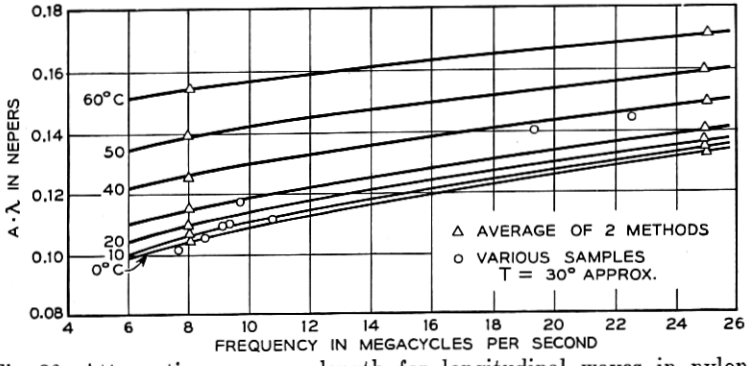

Fig. 36—Attenuation per wavelength for longitudinal waves in nylon 6-6 plotted as a function of temperature and frequency.

points of Fig. 32. Most of the loss is accounted for by shear mechanisms, but it appears that some compressional mechanisms may also be present.

The mechanism causing the relaxation in the megacycle range for polyethylene appears to be the same as for polyisobutylene, namely the relaxation of the shortest chain segment that is free to move. The chain segment acting appears to be longer than six chain units for similar measurements of nylon 6-6 show no relaxations in this frequency range. Fig. 35 shows the longitudinal velocity and Fig. 36 the attenuation per wavelength for longitudinal waves. Since the attenuation per wavelength is still increasing for nylon 6-6 at 25 megacycles a still shorter chain segment may be operating for this material. The shear velocity and attenuation per wavelength for nylon 6-6 are shown by Figs. 37 and 38.

Fig. 39 shows the shear stiffness of polyethylene and nylon 6-6 plotted

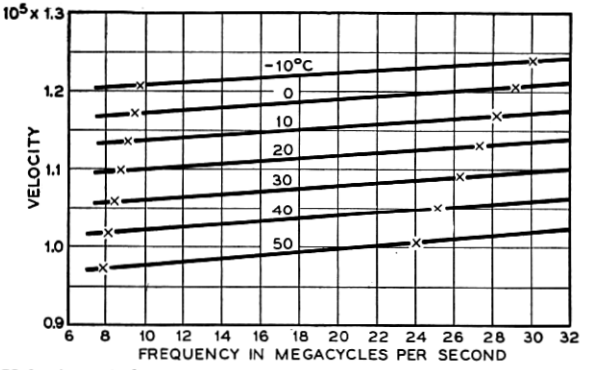

Fig. 37—Velocity of shear waves in nylon 6-6 plotted as a function of temperature and frequency.

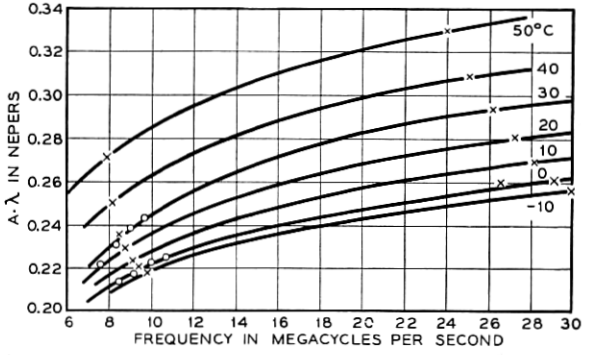

Fig. 38—Attenuation per wavelength for shear waves in nylon 6-6 plotted as a function of temperature and frequency.

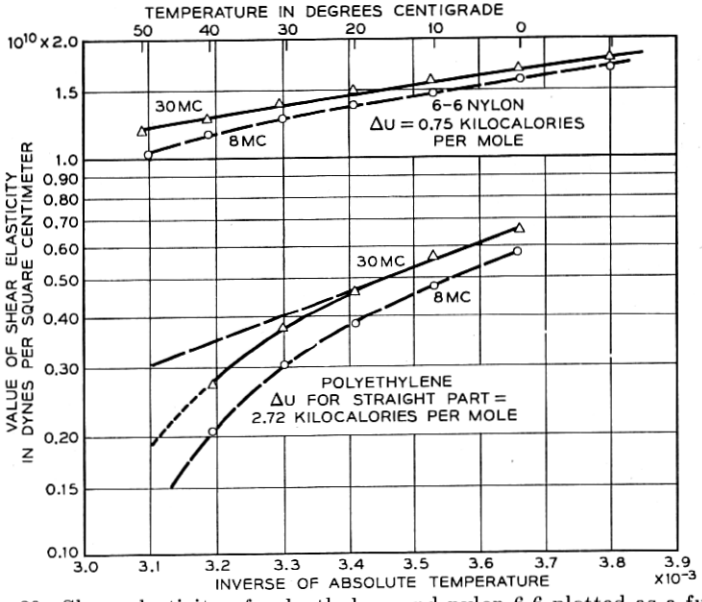

Fig. 39—Shear elasticity of polyethylene and nylon 6-6 plotted as a function of temperature and frequency.

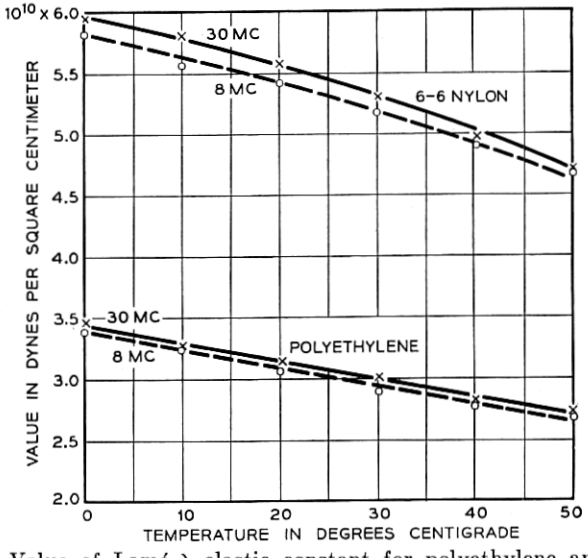

Fig. 40—Value of Lamé λ elastic constant for polyethylene and nylon 6-6 plotted as a function of frequency and temperature.

against $1/T$ where T is the absolute temperature. Both are plotted for 8 mc and 30 mc. The dispersion in both materials is evident. Below 30°C the shear elasticity of polyethylene varies exponentially with the temperature with an activation energy of 2.72 kilocalories per mole. Above this temperature a deviation occurs due to the approach to the melting temperature. Nylon has a smaller variation with temperature.

Comparing the longitudinal and shear wave measurements one can calculate the Lamé λ elastic constant and this is shown plotted on Fig. 40 for both polyethylene and nylon 6-6 as a function of temperature for

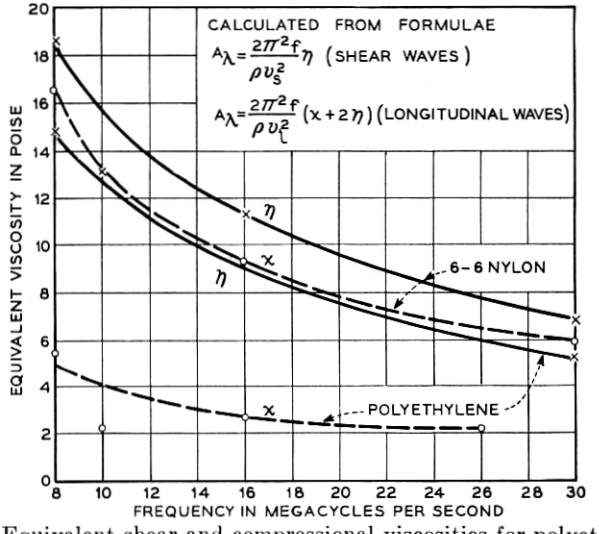

Fig. 41—Equivalent shear and compressional viscosities for polyethylene and nylon 6-6 plotted as a function of frequency for a temperature of 25°C.

two frequencies. The dispersion of λ for polyethylene is small but is more prominent in nylon 6-6. This correlates with the larger compressional viscosity component present for nylon 6-6 which as shown from Fig. 41 is as large as the shear viscosity. According to the structural rearrangement theory of compressional viscosity due to Debye,[16] compressional viscosity can enter when some part of the chain can rearrange from one stable state to another stable state as a function of pressure. This rearrangement occurs across a potential barrier and hence requires a finite amount of time to occur. This lag in the rearrangement results in a compressional viscosity and as the frequency is increased, a frequency is found for which the motion can no longer occur in the time of a single

[16] P. Debye, *Z. Elektrochem.*, **45**, 1939, p. 174.

cycle and the λ constant increases. It appears from these measurements that the dipole binding present in nylon 6-6 allows a greater structural rearrangement under pressure than can occur for polyethylene which has only linear chains.

VI. CONCLUSIONS

Measurements in dilute solutions, in pure polymer liquids and in non rigid solid polymers have all shown the presence of a shortest segment whose relaxation leads to a crystalline type of elasticity. In dilute polymer solutions the presence of a configurational type of relaxation and an entanglement relaxation of the shortest chain segment have been shown. For pure polymer liquids a quasi-configurational type of relaxation has been found for chain lengths greater than 60 segments, but for chain lengths less than 40 segments this type of relaxation disappears. From the difference between the high frequency shear elasticities measured for polyethylene and nylon 6-6 and the static measurement of Young's modulus, it appears that there may be other relaxations in these materials for lower frequency ranges.

For pure polyisobutylene and for nylon 6-6 there appear to be structural changes induced by pressure which account for a compressional viscosity and a dispersion in the λ elastic constant. This effect is smaller for polyethylene.

APPENDIX—EFFECT OF LIQUIDS ON THE PROPAGATION OF SHEAR WAVES IN RODS

For radially symmetric rods, the tangential particle displacement u_θ in the rod is given by

$$u_\theta = J_1(kr)e^{j\omega t - \theta z} \tag{1}$$

where

$$k^2 = \frac{\rho\omega^2}{\mu} + \theta^2 \tag{1A}$$

All other displacements are zero. In this equation waves are considered to be travelling in the $+z$ direction with a propagation constant $\theta = A + jB$, where A is the attenuation in nepers per cm and B the phase shift in radians per centimeter. μ is the shear stiffness which may be complex to take account of the dissipation within the rod.

From the defining relations for the stress strain equation

$$T_{r\theta} = \mu S_{r\theta} = \mu \left(\frac{\partial u_\theta}{\partial r} - \frac{u_\theta}{r} \right)$$

and the tangential particle velocity $\partial u_\theta / \partial t$, one can calculate the impedance Z per square cm. of cylindrical surface at $r = a$. This relation is

$$Z = \frac{-T_{r\theta}}{\dot{u}_\theta} = \frac{j\mu k}{\omega} \left[\frac{J_0(ka)}{J_1(ka)} - \frac{2}{ka} \right] \tag{2}$$

Since only the first mode is excited, parameters can be adjusted to keep k quite small, i.e. ($ka < .2$) and equation (2) can be simplified by using power series expansions for the Bessel functions. Neglecting higher order terms this results in

$$Z = \frac{-j\mu a k^2}{4\omega} \tag{3}$$

To evaluate the impedance of the liquid surrounding the rod, the torsional wave is first propagated along the length of the rod without the liquid, i.e. with $Z = 0$. Then from equation (3) $k = 0$ and from equation (1A)

$$\theta_0^2 = \frac{-\rho\omega^2}{\mu} = (A_0 + jB_0)^2 \tag{4}$$

where A_0 and B_0 are respectively the attenuation and phase shift in the rod alone. With the small loss in metal and glass rods A_0 can be taken equal to zero and

$$B_0 = \omega / \sqrt{\mu/\rho} = \omega / v_0 \tag{5}$$

where v_0 is the velocity of propagation in the rod alone.

When the liquid surrounds the rod, however,

$$k^2 = \frac{\rho\omega^2}{\mu} + \theta^2 = -(A_0 + jB_0)^2 + (A + jB)^2 \tag{6}$$

For the usual case where $(B + B_0) \gg (A + A_0)$, equation (6) approximates

$$k^2 = (B + B_0)(-\Delta B + j\Delta A) \doteq 2B_0(-\Delta B + j\Delta A)$$

where ΔB is the increase in phase shift per centimeter and ΔA the increase in attenuation per cm, both directly measurable quantities. The

final working equation is then given by

$$Z = \frac{\mu a}{4\omega} \times 2B_0[\Delta A + j\Delta B] = \frac{\mu a}{2v_0}(\Delta A + j\Delta B) = \frac{\rho v_0 a}{2}(\Delta A + j\Delta B) \quad (7)$$

Since ΔA and ΔB are the attenuation and phase shift changes per unit length, then if ℓ is the length of the rod, covered the total attenuation and phase shift changes will be ΔA and ΔB multiplied by 2ℓ. Hence if $\overline{\Delta A}_0$ and $\overline{\Delta B}_0$ are the measured attenuation and phase changes, the impedance Z becomes

$$Z = \frac{\rho v_0 a}{4\ell}(\overline{\Delta A}_0 + j\overline{\Delta B}_0) \quad (8)$$

This derivation neglects the change of phase occurring at the intersection between the rod having no liquid and the rod surrounded by the liquid, but it can be shown that this is small and moreover, the change in the wave on leaving is equal and opposite to that occurring on entering and hence this correction cancels out. However, if the liquid is viscous enough there is a correction due to the fact that the measured impedance of equation (8) is for a cylindrical surface, whereas the desired impedance is the characteristic plane wave impedance. Obviously if the radius of curvature is sufficiently large no correction to equation (8) need be made. To obtain a suitable criterion one may consider waves propagated into the liquid from the surface of the rod and solve for the impedance per square cm. of the cylindrical surface. This neglects the variation with z, but since the wavelength along the rod is quite large, little error results from neglecting variations with z.

An outgoing cylindrical wave in the medium may be represented by

$$u_\theta = [J_1(kr)' - jY_1(kr)']e^{j\omega t} = H_1^{(2)}(kr)'\, e^{j\omega t} \quad (9)$$

where the primes refer to the wave in the liquid and

$$(k')^2 = \frac{\rho'\omega^2}{\mu'} = \frac{\rho'^2\omega^2}{Z_k^2} \qquad \text{or} \qquad k'a = \frac{\rho'\omega a}{Z_k} \quad (10)$$

where $Z_k = \sqrt{\mu'\rho'}$ is the plane wave impedance of the liquid.

The shearing stress

$$T_{r\theta} = \mu' S_{r\theta} = \mu'\left[\frac{\partial u_\theta}{\partial r} - \frac{u_\theta}{r}\right],$$

and the tangential velocity may be obtained as before and the complex impedance over the cylindrical surface determined to be

$$Z = \frac{-T_{r\theta}}{\dot{u}_j} = -\mu' \left[\frac{\partial H_1^{(2)}(ka)'}{\partial r} - \frac{H_1^{(2)}(kr)'}{r} \right] \Big/ j\omega H_1^{(2)}(kr)' \quad (11)$$

Noting that for plane waves $Z_k = \sqrt{\rho'\mu'}$, one may eliminate μ' from (11) and evaluate Z at $r = a$ with the result

$$Z = j \left[\frac{H_0^{(2)}(ka)'}{H_1^{(2)}(ka)'} - \frac{2}{(ka)'} \right] Z_k \quad (12)$$

The above equation can be used to obtain a solution for Z_k in terms of the measured value of the cylindrical impedance Z for any set of parameters that may apply. Except for very heavy loading of the rod, however, the results of equation (8) may be used directly with little error. For example calculations indicate that for $| ka |' = 10$, the multiplier of Z_k of equation (12) is approximately $1.07 \angle -7.4°$ for phase angle of $(ka)'$ of $-25°$. For $(ka)' < 10$, the correction multiplier rapidly becomes important. This same correction is applicable for the torsional crystal, but since this is only used for dynamic viscosities less than 10 poises, a correction is seldom necessary.